C.P. No. 759

C.P. No. 759

MINISTRY OF AVIATION

AERONAUTICAL RESEARCH COUNCIL

CURRENT PAPERS

A Free-Flight Investigation of Wing-Body Junction Design for a Transonic Swept-Wing Aircraft

by

G. K. Hunt, B.Sc.(Eng.), A.F.R.Ae.S.

LONDON: HER MAJESTY'S STATIONERY OFFICE

1964

NINE SHILLINGS NET

U.D.C. No. 533.695.12 : 533.6.013.122 : 533.6.011.35

C.P. No.759

August, 1963

A FREE-FLIGHT INVESTIGATION OF WING-BODY JUNCTION DESIGN FOR A TRANSONIC SWEPT-WING AIRCRAFT

by

G. K. Hunt, B.Sc.(Eng.), A.F.R.Ae.S.

SUMMARY

A method of designing the body of a swept wing-body combination, to obtain favourable wing-body interference at transonic speeds, has been investigated in free flight at zero lift. Models of four different bodies, in combination with identical wings swept back 55 degrees, were flown within the range of Mach numbers between 0·8 and 1·5 at Reynolds numbers, based on wing chord, up to 10 million. The general effectiveness of each body shape was determined by measuring the total drag of each model; the local effects of each design were determined by measuring the pressure distribution in the wing-body junction.

The results show that it is possible to design a body which will produce a prescribed velocity distribution in the wing-body junction at a transonic design Mach number, but that it is necessary to control the velocity distribution elsewhere on the wing in order to ensure low drag. An adequate estimate of the overall wave drag is given by linear theory, provided that the Mach number is not too close to unity and the flow on the wing remains shock-free.

Replaces R.A.E. Technical Note No. Aero 2908 - A.R.C. 25,401.

CONTENTS

APPENDICES

ILLUSTRATIONS

1 INTRODUCTION

Several years ago, Bagley[1] discussed the feasibility of designing a swept-wing aircraft that would have a lift/drag ratio of about 13 while cruising at low supersonic speeds. This ratio is higher than had previously been thought to be obtainable at these speeds, and is sufficiently high to make competitive operation of a swept-wing transport aircraft an economic possibility.

The achievement of the required performance will depend on the maintenance of low drag. In particular, the development of wave drag must be deferred to as high a Mach number as possible, and Bagley's analysis depends on the thesis that the wave drag of the wing can be eliminated altogether at low supersonic speeds. He argued that a finite swept wing-body combination can be designed so that the flow everywhere on the wing corresponds very closely to that on an infinite sheared wing. Since the infinite sheared wing may have a supersonic critical Mach number, so too may the finite wing. Thus the performance of this kind of aircraft will depend ultimately on the preservation of the same type of flow on the wing at all Mach numbers at which the aircraft is intended to operate.

One of the important factors affecting the flow over the wing near its root is the shape of the body. Bagley[2] suggested an approximate method of body design, based on quasi-cylinder theory, which was intended to produce a prescribed velocity distribution in the wing-body junction at a specified Mach number. In order to check the method experimentally, a programme of wind-tunnel and free-flight tests was initiated. The free-flight tests, which are the subject of the present paper, were intended primarily to determine the accuracy with which a prescribed velocity distribution could be produced in practice. Since the tests covered a continuous range of speeds, they have also indicated the effectiveness of the method at off-design Mach numbers. In addition the effectiveness of body shapes, designed by the method, in controlling the drag of the wing-body combination has been compared with that of a body designed by means of the supersonic Area rule (see, for example, the review by Sheppard[3]).

Models of four different configurations were flown within the range of Mach numbers between 0·8 and 1·5, at Reynolds numbers up to 10 million based on the mean wing chord. All the configurations had identical swept wings, but one had an unwaisted body, two had waisted bodies designed by Bagley's method and the fourth had an Area-rule body. The overall effectiveness of each design was determined by measuring its total drag, and the local effects of each design were determined from measurements of the pressure distribution in the wing-body junction. The tests were confined to symmetrical configurations at zero lift, and took place during 1958 and 1959.

2 MODEL DESIGN

2.1 The basic model configuration (configuration No.1)

The configuration from which all the free-flight models were derived was that of the swept wing-body combination evolved by Bagley in Ref.1. The basic model configuration consisted simply of this wing-body combination with a stabilising tail unit added. (Figs.1 and 2.)

The wing was swept back 55 degrees and had a gross aspect ratio of 3·40. The trailing edge was straight from root to tip, with a constant chord over the inboard half of the wing and a parabolic leading edge on the outboard half which reduced the chord to zero at the tip. (The ordinates are given in Appendix 1.) This planform was intended to contribute materially to the maintenance of sheared-wing flow. The spanwise distribution of chord resembled that calculated by Brebner[4] for a uniform distribution of C_L across the span in incompressible flow; the tip shape was of the kind deduced by Küchemann and Weber[5] to maintain the sweep of the isobars on the rear part of the outboard chords in subcritical flow. Since Bagley's paper[1] was published, Lock[6] has shown that very similar planforms should have desirable lifting properties near M = 1.

The wing was mounted symmetrically on the body at zero wing-body angle. The uncambered RAE101 aerofoil section was chosen because it has good characteristics at transonic speeds. The thickness/chord ratio of 0·06 was fixed by considerations of model strength and stiffness, and was twice that of the configuration considered by Bagley. For the purpose of the free-flight tests this was probably an advantage, because the effects of a local supercritical flow on the thicker wing should have been more clearly evident in the drag measurements.

The body had an overall slenderness ratio of 16, and its size in relation to the wing was determined by the ratio of body diameter to wing root chord of 0·4, suggested by Bagley. The basic body profile consisted of an ogival nose, a cylindrical centre part and an afterbody which had the same profile as the nose but was truncated to form a finite base. The von Karman ogive was chosen because it is the shape, given by slender-body theory, which has the least wave drag for a given length and base area. (See Appendix 1.)

No attempt was made to represent the kind of tail that might be used on a full-scale aircraft. The tail unit was designed to suit the requirements of a general programme of free-flight tests, of which the tests reported in this paper formed a part. The tailplane had a planform with good structural properties and an orderly movement of its aerodynamic centre through the transonic speed range. The tailplane section was RAE101 with a thickness/chord ratio of 0·04, but the fin section was hexagonal. The leading edges of the fin and tailplane remained subsonic throughout the range of Mach numbers covered by the tests.

2.2 Waisted bodies

The models with waisted bodies were designed by modifying the body of the basic model configuration without altering the wing or the tail.

The principles on which wing-body junction designs must be based, if they are to be fully effective at transonic speeds, were set out by Küchemann and Hartley[7]. First, the critical Mach number of the wing must be raised, if possible to that of the equivalent infinite sheared wing, by restoring the sweep-back of the isobars on the wing near its root. Second, the rate at which the drag rises when the critical Mach number of the wing is exceeded must be reduced to a minimum.

When the critical Mach number of the wing is exceeded, the region of local supersonic flow on the wing is terminated, in general, by a shock. The wing drag rises because the presence of the shock requires a change in the form of the chordwise pressure distribution but, provided the shock is not strong enough to cause separation, the pressure changes are mainly confined to the part of the wing ahead of the shock[8]. Thus the drag rise is related to the position of the shock along the chord, and any design method which controls the rearward movement of the shock will control the rate at which the drag rises. Such a method will only be effective up to Mach numbers near that at which the trailing edge becomes sonic, because the shock will then tend to reach the trailing edge. However, when the wing is swept back 55 degrees the trailing edge does not become sonic until the Mach number is 1·74, and the prospect of controlling the drag at Mach numbers as high as this is attractive and worth investigating.

The critical Mach number and the shock movement can, in principle, be controlled if a prescribed velocity distribution can be achieved over the whole wing in practice. The method of body design suggested by Bagley[2] was intended to determine the velocity distribution only in the region of the wing-body junction. It is assumed that the body is large enough to act as a reflection plate for the wing, and that the velocity in the junction is given with sufficient accuracy by the sum of the velocity due to the body alone and the velocity at the centre section of a wing composed of the nett wing and its reflection. The velocities at the junction due to the wing are calculated, and then a body shape is calculated to produce velocities which, when they are added to the wing velocities, produce the required velocity distribution.

This method was applied to the design of two of the free-flight model configurations. Only the sides of the bodies were waisted, so that the original body depth would be retained, and cross-sections through the waisted parts of the bodies were elliptical. As well as making the assumption that the wing and body flow fields could be superposed, linear theory was used to obtain the velocities and, in the actual calculations, some integrations were replaced by summations. Thus several approximations were introduced, the full significance of which was not known when the models were designed. In addition, each body shape is theoretically correct at only one Mach number, though in practice the required body shape changes slowly with Mach number.

Thus the primary purpose of the free-flight tests was to determine how effectively this method of body design could produce a prescribed velocity distribution in the wing-body junction at the design Mach number. The tests also enabled a comparison to be made between this method and the Area rule, and the effectiveness of both methods to be investigated at off-design Mach numbers.

An obvious starting point, for the process of raising the critical Mach number of the wing to that of the infinite sheared wing, is to try to produce the sheared-wing velocity distribution in the wing-body junction. However, the body shape calculated to achieve this on the free-flight model, at a design Mach number of 1·2, reduced the body width by half at the wing-root trailing edge, and the body sides continued to converge aft of the wing root (Fig.3). This design was, therefore, abandoned and other shapes were

designed which were considered sufficiently practicable to be tested in free flight. These are described in the following sections, and their ordinates are given in Appendix 2.

2.2.1 Configuration No.2

The body of this configuration was designed to produce, at M = 1·2, a velocity distribution different from that on the infinite sheared wing. The suction peak was farther forward and the velocities at all points aft of the suction peak were reduced. (Fig.3) The body indentation was less severe than that calculated to achieve the full sheared-wing distribution, and the body sides diverged slightly at the wing-root trailing edge, but the maximum body width was not restored within the length of the model (Fig.4).

The shape of the calculated velocity distribution implies that, provided sheared-wing flow is established farther out on the wing, the isobars forward of the peak suction line should have the required sweep of 55 degrees and the isobars aft of the peak suction line should be swept back even more. Thus, under these conditions, the critical Mach number should be at least as high as that of the sheared wing. However, when the velocity distribution is compared with that on the sheared wing, it is clear that in this case there is less suction on the forward-facing part of the wing near the root and more pressure on the forward-facing part of the body waist. Thus, although the flow in the wing-body junction should be shock-free, the drag may be greater than that of a configuration designed to maintain sheared-wing flow in the junction.

When the critical Mach number of a wing has been exceeded, the local Mach number just ahead of the wing shock may become almost independent of the flight Mach number until the trailing edge becomes sonic. (See, for example, Refs.8 and 9.) There may, therefore, be a lower limit to the Mach number just aft of the shock. If the local Mach numbers on the rear of the wing are reduced by body design, the rearward movement of the shock should be slowed down. The reduction of all velocities aft of the suction peak on the wing of this model configuration should, therefore, reduce the rate at which the wing shock moves rearward when the critical Mach number is exceeded, and the rate at which the drag rises should be lower than for the infinite sheared wing.

2.2.2 Configuration No.3

The body of this configuration was subject to the practical limitation that the minimum body width should not be less than three-quarters of the full body diameter (Figs.3 and 4). It was shaped so that, at the design Mach number of 1·2, the suction peak would be as far forward as on configuration No.2, though full sheared-wing suction could not be developed with such a moderate waist. The calculated rate of pressure recovery aft of the suction peak is less than on configuration No.2 but the velocities are all lower than on the infinite sheared wing.

The fact that the calculated suction peak in the wing-body junction is lower than that on the sheared wing means that, if sheared-wing flow is established farther out on the wing, some of the isobars on the wing will form closed loops. However, the unswept parts of the loops should be forward of

the peak suction line. Behind this line the isobars should all be swept more than 55 degrees and, as it is in this region that the wing shock occurs, the critical Mach number should still be at least as high as that of the sheared wing. The drag, like that of configuration No.2, may be higher than if sheared-wing flow had been produced in the wing-body junction, even when the flow there is shock-free. When the critical Mach number is exceeded the reduced velocities on the rear of the wing should delay the drag rise, in the same way as on configuration No.2.

2.2.3 Configuration No.4

The body of this configuration had the same length, volume and base area as the basic, unwaisted body, but the volume was redistributed in accordance with the Transfer-rule version of the supersonic Area rule[3].

Experience of the supersonic Area rule had indicated that, while it may be successful in maintaining low wave drag at the design Mach number, it may be less effective at other Mach numbers and that, as a result, a drag peak may occur at sonic speed. Therefore, although the intended cruise Mach number of this configuration remained 1·2, its design Mach number was reduced to 1·16. It was hoped thereby to flatten the supersonic part of the drag curve, up to M = 1·2, by reducing the sonic peak while incurring only a trivial penalty at the design Mach number.

The wing-body combination was treated in three parts: a von Karman ogive with the length and base area of the body, the additional body volume, and the volume of the exposed wing (Fig.5(a)). The additional volume of the basic body was first redistributed until, at M = 1·16, the mean oblique area distribution of the combined additional body volume and transferred wing volume was that of a Sears-Haack body. The area distribution of the resultant waisted body was then obtained by subtracting the transferred area distribution of the exposed wing from the new total area distribution of the wing-body combination. The rear part of this body was rather narrow and would have restricted the installation of standard telemetry components in the free-flight model. A partially-waisted body was therefore adopted. Its cross-section areas differed from those of the unwaisted body by only 60 per cent of the amounts required by the Area rule (Fig.5(b)). Calculations by Lord, based on an extension to the Transfer rule of the results for the sonic Area rule reported in Ref.10, indicated that this body should achieve 84 per cent of the drag reduction that the fully-waisted body would achieve.

As the Transfer rule does not impose any restriction on the shapes of body cross-sections, the model was designed to have a body of revolution in order to simplify its manufacture.

3 EXPERIMENTAL TECHNIQUE

The bodies of the models were designed specifically for zero lift conditions. Therefore, prior to the free-flight tests, the tailplane angle to trim the models at zero lift was determined from tests in the 8 ft × 8 ft supersonic wind tunnel at the R.A.E., Bedford and in the 9 ft × 8 ft transonic tunnel of the Aircraft Research Association, Ltd.

The model used in the tunnel tests was identical in size and shape to the free-flight Area-rule model in all respects except the shape of the rear end of the body. This was cylindrical instead of tapered in order to admit a rear sting support. The tunnel tests indicated that, at zero lift, there was a downwash angle of about one degree at the tailplane position, at all Mach numbers to be covered by the free-flight tests. Accordingly the tailplanes of the free-flight models were set at a positive angle of one degree, and the flight tests confirmed that this was correct.

The models were flown at the Larkhill range. Three models of the basic (unwaisted) configuration were flown, and one model of each of the waisted configurations. Boundary-layer transition was allowed to occur naturally on all the models. Each model was launched from the ground by twin rocket motors (Fig.6b) and reached its maximum velocity in about $3\frac{1}{2}$ seconds. The rocket motors were detached as soon as they stopped thrusting, and the experimental measurements were made while the model was decelerating in free flight. The models followed a fairly low trajectory, and in order that they should not fly beyond the limits of the range each model was destroyed in the air by an explosive charge, detonated by a clockwork time fuse.

Every model carried standard RAE465 Mc/s telemetry equipment. The lateral, longitudinal and normal components of the acceleration of the model were measured at its centre of gravity, and the normal accelerations were also measured at points near the nose and tail so that longitudinal stability could be investigated if necessary. With the exception of one of the unwaisted models, static pressures were measured at 14 points in the wing-body junction of each model. The flight path of each model was determined from measurements made by synchronised kine-theodolites at several stations along the range. Velocity was determined by radio-Doppler measurements.

The first models to be flown were those of configurations 3 and 4, and their results showed that neither model had reached subsonic speeds. In order that the remaining models should do so, their weights were reduced and their flight times were increased from 18 to 22 seconds by re-setting the time fuses. As the tests progressed, it became clear that the drag rise of the models was starting at a lower Mach number than had been expected, and that the models were still not reaching a low enough Mach number, before being destroyed, to enable the subsonic drag level to be measured. Therefore, before the last unwaisted model was fired it was installed in the 13 ft x 9 ft wind tunnel at R.A.E., Bedford, and its zero-lift drag was measured at speeds of 200 and 300 feet per second. (Fig.6a.) When this model was flown, its maximum velocity was reduced by adding ballast to the rocket motors that launched it, with the object of confirming both the subsonic drag level and the shape of the drag rise.

4 DISCUSSION OF RESULTS

4.1 Interpretation of the results

At least a week elapsed between the calibration of a set of pressure transducers and the flight of the model containing them. During this period, the zero-pressure level indicated by some of the transducers drifted slightly.

The drift of each instrument was measured on the range just prior to firing, and appropriate corrections were applied during analysis of the results. However, their effect has been to make the uncertainty in the absolute pressures indicated by any single transducer greater than the uncertainty in the indicated changes of pressure. The estimated maximum uncertainties are indicated in Figs.8, 9 and 10.

Drag measurements were obtained from the accelerometers carried in the models, and by differentiation of the radio-Doppler velocity measurements made on the ground. Though the Doppler measurements indicate drag levels accurately, they are incapable of resolving rapid fluctuations of drag. They have, therefore, been regarded only as a means of checking the accelerometer measurements, and they are not presented in this report for those models from which accelerometer measurements were obtained. It is worth recording that, in every case, the drag levels indicated by the accelerometers were confirmed by the Doppler results within the accepted uncertainty limits for tests of this kind. The greatest uncertainties in the drag measurements are ± 4 per cent at supersonic speeds and ± 12 per cent at subsonic speeds.

It should, perhaps, be pointed out that the severe drag rise experienced by all the models at high subsonic speeds is not typical of this wing-body combination. More than half the drag rise is associated with the tail unit, which was designed primarily to satisfy engineering requirements.

The models were manufactured within a dimensional tolerance of ±0·003 inch on all the ordinates of the external surfaces.

4.2 Configuration No.1 (no waist)

The pressure distribution in the wing-body junction of configuration No.1 was measured on two models and the results are presented in Fig.8.

There is some scatter of the experimental points, but the results show clearly that the shape of the pressure distribution changed continuously from its subsonic form to a typically supersonic form at subsonic Mach numbers. At Mach numbers greater than 0·9 there was a sharp pressure rise at the wing root trailing edge, probably caused by a shock, and at sonic flight speed fully supersonic flow was established in the wing-body junction.

Results were obtained from only one model (model A) at M = 1·2. At this Mach number the pressure rise at the trailing edge agreed closely with the estimate, but the pressures measured elsewhere on the wing root chord were generally higher than the estimated values. At lower Mach numbers the pressures on the second model (model B) were generally lower than those on model A, and it seems likely that this tendency would have persisted at M = 1·2. Thus had results been obtained from model B at M = 1·2 they would probably have been nearer to the estimated values than those actually obtained from model A. Some of the difference between the measured and the estimated pressure distributions may be due to the slight natural waist which is formed when a wing of finite thickness intersects a cylindrical body.

The reason for the lack of agreement between the pressure measurements from the two models is not known. It is not due to a difference of C_L,

because both models were within 0·002 of the same C_L at all Mach numbers, whereas the measured differences in C_p require a difference in C_L of about 0·05. Both models rolled very slowly in flight, but they rotated in the same direction and at almost the same rate. There were slight differences between the indicated lateral accelerations of the models, but they were so small as to be well within the estimated uncertainty of the measurements. The records of the telemetry signals received from the two models are of good quality. Inspection records show that both models were within the dimensional tolerance of ±0·003 inch at all points, and that errors in one model tended to appear in the same place on the other. Thus the difference between the shapes of the two models was very small and is unlikely to have contributed appreciably to the measured pressure differences.

The drag of configuration No.1 was measured on three models, two of which were also used to obtain pressure measurements. The results are presented in Fig.11(a). The symbols used in this Figure, to distinguish between the models, correspond to those used in Fig.8. Although there is a slight difference in level between the three curves at supersonic speeds, this is within the estimated uncertainty of the experimental results. There is very little scatter of the experimental points from any particular model, and the three curves define the shape of the drag curve clearly at supersonic speeds.

At subsonic speeds models A and B yielded two distinct curves, with model C following first one curve and then the other. The two separate curves on their own might have been suspect, but the jump from one curve to the other made by model C suggests that both curves may be genuine, and that the difference between them may be due to a boundary-layer effect.

4.3 Configuration No.2 (severe waist)

The pressure distribution in the wing-body junction of configuration No.2 was measured on one model, and the results are presented in Fig.9. They appear to have less scatter than the results obtained from the models of configuration No.1, and show quite clearly that the pressure distribution in the junction remained essentially subsonic in character and shock free up to $M = 1·45$, the highest Mach number achieved by this model. The form of the pressure distribution remained remarkably constant, and it would appear that completely shockless flow was achieved in the junction throughout the Mach-number range covered by the test. The resemblance between the prescribed pressure distribution and the measured distribution at $M = 1·2$ is good, and there can be no doubt that the design method has been generally successful.

It is, however, worth noting that the measured suction peak at $M = 1·2$ was not as high or as far forward on the wing chord as the peak of the prescribed distribution, and that in general the measured pressures were a little higher than the corresponding prescribed pressures. Thus there was less suction on the front of the wing, but more pressure on the rear, so the drag of the wing near the root was probably not very different from the drag associated with the prescribed distribution. The occurrence of the suction peak aft of the prescribed position suggests that the isobars on the wing forward of the

suction peak may not have maintained the full sweep-back of 55 degrees. This is not important in this particular case, as the suction peak was still well forward of the crest of the wing section.

The drag of configuration No.2 was measured on the model that was used for the pressure measurements, and the results are presented in Fig.11(b). The drag-rise Mach number appears to be higher than that of configuration No.1, and since the flow in the wing-body junction was shockless this is to be expected. The drag-rise Mach number should be that of the body and tail alone. At low supersonic Mach numbers the drag was certainly lower than that of configuration No.1, but at M = 1·1 the drag rose quite sharply and continued to rise as the Mach number increased, without any corresponding change of trim or of the form of the pressure distribution in the wing-body junction. There is no evidence to show why this happened, but there can be little doubt that it did so. The results show some scatter, but the same trend is followed by drag measurements from three sources: longitudinal accelerometers in the model, and kinetheodolites and radio-Doppler equipment on the ground. High-speed cine films indicate that the model was intact throughout its flight.

4.4 Configuration No.3 (moderate waist)

Only one model of this configuration was flown, and its telemetry transmitter failed one second after it left the ground. Therefore no measurements of pressures or accelerations were obtained from the model itself. The drag of the model at supersonic speeds was derived from radio-Doppler velocity measurements only, and these results are presented in Fig.11(c). The general level of the drag was considerably lower than that of configuration No.2 in the same Mach-number range (Figs.12 and 13) and the sharp drag rise at M = 1·1, associated with configuration No.2, did not occur. The drag of configuration No.3 may be slightly lower than that of the unwaisted configuration (No.1), but the difference in level between the curves is of the same magnitude as the estimated uncertainty of the measurements.

4.5 Configuration No.4 (Area rule)

The pressure distribution in the wing-body junction of configuration No.4 was measured on one model at supersonic speeds only, and the results are presented in Fig.10. The curves show clearly that the shape of the pressure distribution remained almost constant throughout the Mach-number range covered by the test, and was essentially subsonic in form.

Compared with configuration No.2, the wing-root of configuration No.4 had less suction over the forward part and more suction over the rear part. The drag of the wing near the root must, therefore, have been greater than on configuration No.2, though less than on configuration No.1. At M = 1·2 the suction peak was lower than that calculated for the infinite swept wing, and at all Mach numbers the suction peak occurred aft of the crest of the wing-root section. If sheared-wing flow developed farther out on the wing, some of the isobars must have formed closed loops near the wing-root, and the isobars forward of the peak suction line could not have been fully swept. However, the measured pressures aft of the suction peak agree very closely at M = 1·2 with the calculated pressures on the infinite sheared-wing, so the full sweep-back of the isobars on the wing aft of the suction peak was probably just maintained.

A curious feature of the measured pressure distributions is the strong suction peak just forward of the wing-root trailing edge. This may be genuine, but it could be due to a faulty transducer or, possibly, to damage sustained when the rocket motors separated from the model. Such damage is extremely unlikely, but it cannot be discounted in this case because there was an aerial slot, filled with synthetic resin, in the wing near the trailing edge. If the resin had become dislodged it would have produced a disturbance where the measured suction peak occurred.

The pressure distribution in the wing-body junction of this configuration was calculated at two Mach numbers by means of linear theory. The calculations agree well with the measurements, though the measured pressures are, in general, higher than the calculated pressures, and the measured suction peaks are slightly aft of the calculated ones. There is a discontinuity in the calculated pressure distribution at the wing root trailing edge, and there is a sharp rise at this point in the measured pressure distributions. The picture is confused by the indicated suction peak just ahead of the trailing edge, but the calculations are at least confirmed qualitatively.

The drag of configuration No.4 was measured on the model that was used for the pressure measurements, and the results are presented in Fig.11(d). The curve is well defined, and shows a slight dip near $M = 1{\cdot}2$ followed by a distinct rise near $M = 1{\cdot}25$. The drag curve correlates qualitatively with the pressure measurements, to the extent that the drag level changes only slightly throughout the Mach number range covered by the test. The comparison of all the drag results in Fig.12 suggests that the drag of configuration No.4 is lower than that of configuration No.1, though the difference in levels is of the same magnitude as the maximum experimental uncertainty. Contrary to the indications of the pressure measurements, the drag of configuration No.4 is not higher than that of configuration No.2, except perhaps near $M = 1{\cdot}1$.

These results suggest that, although the body of this configuration was not designed to produce a prescribed flow in the wing-body junction, it maintained the sweep-back of the isobars on the rear of the wing, and hence shockless flow; it also had fairly low drag throughout a range of Mach numbers on either side of the design Mach number. Measurements from the corresponding fully-indented Area-rule configuration would have made an interesting comparison.

4.6 General comments

The pressure distribution measured in the wing-body junction of configuration No.2 at the design Mach number was reasonably close to the prescribed pressure distribution. The principal difference was that the actual suction peak occurred about 10 per cent farther aft on the chord than the prescribed peak. In addition linear theory has predicted the shapes of the pressure distributions in the wing-body junctions of the unwaisted configuration and the Area-rule configuration, though there are some discrepancies in the magnitudes of the pressures. Thus in all three cases the method of design suggested by Bagley has been a reliable guide to the form of the flow in the wing-body junction, and it has yielded good quantitative estimates for the configurations with waisted bodies. Therefore it can be said that the method provides a good starting point for the prediction or definition of the pressure distribution in a wing-body junction.

The relationship between the pressure distribution in the wing-body junction and the drag of the wing-body combination remains uncertain. If the rise in the measured drag of configuration No.2, which occurred at about $M = 1 \cdot 1$, is genuine it implies that the beneficial effects of the body design on the flow near the wing root are more than counterbalanced by adverse effects elsewhere. The other configurations develop a more moderate drag rise at slightly higher Mach numbers, but still without any appreciable changes of trim or of the form of the pressure distribution in the wing-body junction. Thus the achievement of shock-free flow in the junction is not sufficient by itself to ensure low drag.

All the drag measurements for the complete models are summarised and compared with the estimated friction and wave drag in Fig.12. Although this Figure shows that the estimates and measurements agree quite well, it may give a misleading impression of the relative magnitudes of the drag measurements because they include a large contribution from the tail. Estimates of the tail drag, which have been confirmed by transonic tunnel tests[11], were subtracted to obtain drag curves for the wing-body combinations and these are presented in Fig.13.

Wave-drag curves for the wing-body combinations are of particular interest, since one of the principal objects of body design at transonic speeds is the minimisation of wave drag. They are presented in Fig.14, and were obtained by subtracting the estimated friction drag of the wing and body from the values plotted in Fig.13. The greatest uncertainty in the values of wave drag is ±6 per cent, though the actual errors are probably much less than this. In Fig.15 the wave drag is expressed in terms of the factor K_o, which is the ratio of the wave drag of a given configuration at zero lift to that of a Sears-Haack body with the same length and volume. It can be regarded as an index of volumetric efficiency. The relative positions of the curves in Fig.15 differ from those in Fig.14 because configurations 2 and 3 were designed by removing volume from the body of configuration No.1. Theoretical values of K_o, calculated by means of linear theory, are plotted in Fig.15 for comparison.

Two important points emerge from Fig.15. The first is that the unwaisted wing-body combination had 35 per cent more wave drag at its design Mach number than the equivalent Sears-Haack body. Efforts to reduce this excessive wave drag are obviously well worth while. The Area rule body achieved some reduction, and it is likely that greater reductions could be achieved by calculating the flow in some detail in the manner indicated by Bagley. The fact that configurations 2 and 3 did not reduce the wave drag factor below that of the unwaisted body at the design Mach number is not significant, because they were not intended specifically to do this. The second point is that, at the design Mach number, the values of K_o calculated by means of linear theory are generally in the correct sequence. The exception is configuration No.2, whose very high measured drag remains unexplained. At low Mach numbers the theory becomes progressively less reliable until, at sonic speed, it indicates infinite wave drag. At high Mach numbers the theory remains reliable only up to the critical Mach number of the wing, since it does not take account of shocks.

5 CONCLUSIONS

(a) A method of designing the body of a swept wing-body combination, to produce favourable wing-body interference at transonic speeds, has been suggested by Bagley[1]. Linear theory is used to calculate the separate contributions from the wing and the body to the flow in the wing-body junction; in calculating the flow due to the wing it is assumed that the side of the body acts as an infinite reflection plane.

Measurements made in free flight indicate that the method is adequate, either to obtain the shape of the body which will produce a prescribed velocity distribution in the wing-body junction or to indicate the velocity distribution in the junction of an existing wing-body combination. In particular, when the method predicted shockless flow the measurements indicated that the flow was in fact shockless.

(b) None of the four different wing-body combinations which were investigated in free flight was intended to achieve sheared-wing flow in the wing-body junction. As a result they may have developed some drag on the wing near the root and on the waisted part of the body, even when the flow in the junction was shockless. In spite of this, linear theory provided good estimates of their overall wave drag and, with one unexplained exception, indicated the correct relative magnitudes. This is important because it may not always be possible to design practical full-scale aircraft to have sheared-wing flow in the wing-body junction. The theory is, of course, not valid near sonic speed or above the critical Mach number of the wing.

(c) An advantage obtained by good body design is shown clearly by expressing the wave drag of each wing-body combination as a multiple of the wave drag of the Sears-Haack body with the same length and volume, in terms of the factor K_o. At their design Mach number of 1·2 all the configurations had a K_o greater than unity but, while the factor for the unwaisted configuration was 1·35, that for one of the waisted configurations derived from it was 1·15. Thus a considerable reduction in wave drag was achieved by body design.

(d) The free-flight measurements show that the achievement of shockless flow in the wing-body junction is not sufficient by itself to ensure low drag. Therefore, in designing for low drag at transonic speeds, it is necessary to produce a prescribed velocity distribution not only in the wing-body junction but also elsewhere on the wing. The effect of variations in body shape on the overall wave drag can be determined by means of linear theory. It is very unlikely that any of the bodies of the free-flight models was a true optimum, and lower values of K_o should be attainable for wing-body combinations. They are well worth striving for, since the most difficult part of the problem has already been solved, namely the achievement of shockless flow in the wing-body junction in supersonic flight.

SYMBOLS

A	aspect ratio of gross wing
B	base area of the nose ogive
c	local chord
c_o	centre-line chord of the gross wing
$\bar{c}$	aerodynamic mean chord of the gross wing $= \dfrac{\int c^2\, dy}{\int c\, dy}$
C_{D_o}, C_{D_W}, C_L	zero-lift drag coefficient, wave drag coefficient, lift coefficient $= \dfrac{\text{Force}}{\frac{1}{2}\gamma p_s M^2 S}$
C_p	pressure coefficient $= \dfrac{p - p_s}{\frac{1}{2}\gamma p_s M^2}$
K_o	ratio of the zero-lift wave drag of a given configuration to that of a Sears-Haack body with the same length and total volume $= C_{D_W} S \times \dfrac{\pi L^4}{128 V^2}$
ℓ	length of the nose ogive
L	total length of a configuration
M	Mach number
Mc/s	megacycles per second
p	local static pressure
p_s	static pressure of undisturbed air
r	local radius of the body
Re	Reynolds number (here based on $\bar{\bar{c}}$)
s	semi-span of the gross wing
S	area of the gross wing (used here as the reference area)
$S(x)$	area of a normal cross-section at station x

SYMBOLS (CONTD)

u	difference between the local velocity component in the x-direction and the flight velocity
U	velocity of flight
V	total volume of a configuration
x,y	rectangular coordinates in the plane of the wing; x along the body axis, y spanwise
γ	ratio of the specific heats of air, assumed to 1·40
Λ	leading-edge sweep-back angle

REFERENCES

No.	Author	Title, etc.
1	Bagley, J.A.	An aerodynamic outline of a transonic transport aeroplane. ARC 19,205. October 1956.
2	Bagley, J.A.	Some aerodynamic principles for the design of swept wings. Progress in Aeronautical Sciences, Vol.3. Pergamon Press, 1962.
3	Sheppard, L.M.	Methods for determining the wave drag of non-lifting wing-body combinations. ARC R & M No.3077. April 1957.
4	Brebner, G.G.	The design of swept wing planforms to improve tip-stalling characteristics. RAE Report No. Aero 2520. ARC 17,264 July 1954.
5	Küchemann, D. Weber, J.	The subsonic flow past swept wings at zero lift without and with body. ARC, R & M No.2908. March 1953.
6	Lock, R.C.	The design of wing planforms for transonic speeds. Aero. Quart 12(1). February 1961.

REFERENCES (CONTD)

No.	Author	Title, etc.
7	Küchemann, D. Hartley, D.E.	The design of swept wings and wing-body combinations to have low drag at transonic speeds. RAE Report No. Aero 2537. ARC 17,869. April 1955.
8	Küchemann, D.	Methods of reducing the transonic drag of swept-back wings at zero lift. Jnl. R. Ae. Soc. 62(565) January 1957.
9	Sinnott, C.S. Osborne, J.	Review and extension of transonic aerofoil theory. ARC R & M No.3156. October 1958.
10	Lord, W.T.	On the design of wing-body combinations of low zero-lift drag rise at transonic speeds. ARC R & M No.3279. October 1959.
11	Haines, A.B. Jones, J.C.M.	Transonic tunnel tests on a 6% thick, warped 55° sweptback wing model. Aircraft Research Association Wind Tunnel Note No.25, September 1960.
12	Pankhurst, R.C. Squire, H.B.	Calculated pressure distributions for the RAE 100-104 aerofoil sections. ARC C.P.80. March 1950.
13	Low, G.M.	Boundary-layer transition at supersonic speeds. NACA Res. Memo. E56 E10. (NACA/TIL/5205) (ARC 19,043). August 1956.
14	Weber, J. Brebner, G.G.	A simple estimate of the profile drag of swept wings. RAE Tech. Note No. Aero 2168. ARC 15,246. June 1952.
15	Eminton, E.	On the minimisation and numerical evaluation of wave drag. RAE Report No. Aero 2564. ARC 19,212. November 1955.
16	Fraenkel, L.E.	The theoretical wave drag of some bodies of revolution. ARC R & M No.2842. May 1951.

REFERENCES (CONTD)

No.	Author	Title, etc.
17	Bishop, R.A. Cane, E.G.	Charts of the theoretical wave drag of wings at zero lift. ARC C.P.313. June 1956.
18	Brebner, G.G. Lord, W.T.	Some properties of curved planforms for sweptback wings at subsonic and supersonic speeds. RAE Tech. Note No. Aero 2417. ARC 18,315. November 1955.

APPENDIX 1

GEOMETRY OF THE BASIC WING-BODY COMBINATION
(Configuration No.1)

The basic configuration had a body of revolution made up of an ogival nose, a cylindrical centre portion, and an afterbody which had the same profile as the nose but was cut off where its diameter was one inch. The ogive had the shape, given by slender-body theory, which has the least wave drag for a given length and base area. (The von-Karman ogive.) Its profile is given by

$$r = \left(\frac{S(x)}{\pi}\right)^{\frac{1}{2}}$$

where
$$S(x) = \frac{2B}{\pi}\left\{\sin^{-1}\left(\frac{x}{\ell}\right)^{\frac{1}{2}} + \left(2\frac{x}{\ell} - 1\right)\left[\frac{x}{\ell}\left(1 - \frac{x}{\ell}\right)\right]^{\frac{1}{2}}\right\}$$

and
$$0 \leq \frac{x}{\ell} \leq 1 .$$

Ordinates of the models, calculated in inches by means of these expressions, are given in the following table:

TABLE 1 - Ordinates of the basic body

Inches aft of nose tip	Body radius (inches)	Inches forward of after-body base
0	0	
1	0.266	
2	0.446	
2.340	0.500	0
3	0.600	0.660
4	0.740	1.660
5	0.870	2.660
6	0.991	3.660
7	1.105	4.660
8	1.214	5.660
9	1.317	6.660
10	1.416	7.660
11	1.510	8.660
12	1.600	9.660
13	1.686	10.660
14	1.768	11.660
15	1.846	12.660
16	1.921	13.660
17	1.993	14.660
18	2.060	15.660
19	2.125	16.660
20	2.186	17.660
21	2.242	18.660
22	2.295	19.660
23	2.344	20.660
24	2.388	21.660
25	2.427	22.660
26	2.460	23.660
27	2.486	24.660
28	2.500	25.660

Appendix 1

The wing planform was defined as follows. The trailing edge was straight from root to tip and was swept back 55°. The inboard half of the wing had a constant chord and the spanwise distribution of chord over the outboard half of the wing was defined by

$$c = 2c_o \left\{ \left[2\left(1 - \frac{y}{s}\right) \right]^{\frac{1}{2}} - \left(1 - \frac{y}{s}\right) \right\}$$

where $$0{\cdot}5 \leq \frac{y}{s} \leq 1{\cdot}0 \ .$$

Chords of the models, calculated by means of this expression, are given in the following table.

TABLE 2 - Ordinates of outboard half of wing planform

y inches	$\frac{y}{s}$	$\frac{c}{2c_o}$	c inches
9·739	0·50	0·50	12·500
10·0	0·5134	0·4999	12·498
10·5	0·5390	0·4992	12·480
11·0	0·5647	0·4977	12·443
11·5	0·5904	0·4955	12·388
12·0	0·6161	0·4924	12·310
12·5	0·6417	0·4882	12·205
13·0	0·6674	0·4830	12·075
13·5	0·6931	0·4766	11·915
14·0	0·7188	0·4687	11·718
14·5	0·7444	0·4594	11·485
15·0	0·7701	0·4482	11·205
15·5	0·7958	0·4349	10·873
16·0	0·8214	0·4191	10·478
16·5	0·8471	0·4001	10·003
17·0	0·8728	0·3772	9·430
17·5	0·8985	0·3491	8·728
17·75	0·9113	0·3326	8·315
18·0	0·9241	0·3137	7·843
18·25	0·9370	0·2920	7·300
18·5	0·9498	0·2667	6·668
18·75	0·9626	0·2361	5·903
19·0	0·9755	0·1969	4·923
19·125	0·9818	0·1724	4·310
19·25	0·9883	0·1413	3·533
19·375	0·9947	0·0981	2·453
19·479	1·0	0	0

The wing section was RAE101, with a thickness/chord ratio of 0·06. Ordinates of this section are given in Ref.12.

APPENDIX 2

GEOMETRY OF THE WAISTED BODIES

Configurations No.2 and 3 were waisted only in planform, and retained in elevation the profile of configuration No.1. In the following table, ordinates are given for only the planforms of the waisted parts of the bodies. Cross-sections through the waisted parts were half-ellipses, separated by the local wing thickness; elsewhere the cross-sections remained circular.

TABLE 3 - Ordinates of the waists of configurations No.2 and 3

Inches aft of nose	Body half-width (inches)	
	Config. No.2	Config. No.3
32	2·452	2·466
33	2·324	2·376
34	2·160	2·266
35	2·000	2·150
36	1·860	2·048
37	1·740	1·964
38	1·656	1·906
39	1·608	1·876
40	1·592	1·870
41	1·603	1·890
42	1·648	1·936
43	1·734	2·006
44	1·790	2·086
45	1·846	2·156
46	1·904	2·223
47	1·959	2·291
48	2·014	2·356
49	2·070	2·406
50	2·126	2·444
51	2·185	2·473
52	2·239	2·494
53	2·294	
54	2·350	same as
55	2·404	config.
56	2·435	No.1
57	2·434	

Configuration No.4 had a body of revolution, designed by means of the Area rule to have the same length, volume and base area as the body of the basic, unwaisted configuration (configuration No.1).

TABLE 4 - Ordinates of the body of configuration No.4

Inches aft of nose	Body radius (inches)
0	0
1	0·288
2	0·486
3	0·659
4	0·816
5	0·960
6	1·093
7	1·216
8	1·331
9	1·439
10	1·540
11	1·635
12	1·725
13	1·810
14	1·890
15	1·966
16	2·038
17	2·107
18	2·172
19	2·234
20	2·292
21	2·347
22	2·399
23	2·448
24	2·496
25	2·538
26	2·579
27	2·616
28	2·650
29	2·679
30	2·703
31	2·719
32	2·724
33	2·710
34	2·678
35	2·631
36	2·573
37	2·512
38	2·457
39	2·411
40	2·375

Inches aft of nose	Body radius (inches)
41	2·349
42	2·332
43	2·323
44	2·319
45	2·319
46	2·321
47	2·323
48	2·325
49	2·326
50	2·326
51	2·324
52	2·320
53	2·312
54	2·301
55	2·286
56	2·266
57	2·242
58	2·213
59	2·179
60	2·141
61	2·098
62	2·051
63	1·999
64	1·943
65	1·883
66	1·819
67	1·751
68	1·679
69	1·604
70	1·525
71	1·443
72	1·356
73	1·264
74	1·165
75	1·058
76	0·940
77	0·815
78	0·690
79	0·573
80	0·500

APPENDIX 3

NOTE ON DRAG ESTIMATES

All the estimates relate to the basic, unwaisted configuration.

(a) Skin friction

A simple approach was made to the problem of estimating skin friction on the free-flight models used in these tests. Boundary-layer transition was assumed to occur on the body in flight at a Reynolds number of 10 million at all Mach numbers. In the 13 ft x 9 ft wind tunnel, transition on the body was assumed to occur 28 inches aft of the nose, at the point where the nose ogive joined the cylindrical part of the body. In the tunnel, the Reynolds numbers at this point were 3 million at 200 ft/sec and 4·5 million at 300 ft/sec.

Transition positions, rather than transition Reynolds numbers, were selected separately for the wing, tailplane and fin, and these positions were regarded as invariant with Mach number. On an unswept RAE101 aerofoil at the scale of the free-flight tests, transition might be expected to occur near the crest of the section, but the effect of leading-edge sweep is to move the transition point forward. For the estimates presented in this paper the fraction of the chord at which transition occurred on the swept surfaces was taken to be $\cos^3\Lambda$ times that on the corresponding unswept wing, as suggested in Ref.13. The friction was obtained from R.Ae.S. data sheets, treating the wing and the tailplane as flat plates, but some account of the effect of sweep on the flow in the boundary layer was taken by using the result of Ref.14. This shows that the friction drag coefficient of a swept surface at a Reynolds number Re is cos Λ times the drag coefficient of an unswept surface with the same chord, at a Reynolds number Re $\cos^2\Lambda$. (Transition is assumed to occur at the same fraction of the chord on the swept and the unswept surfaces.)

Transition on the fin was assumed to occur at the first ridge line, where the Reynolds number was about 2·5 million at M = 1·2. This is a likely transition Reynolds number on a wedge, and the sharp ridge would almost certainly cause transition if it had not already occurred. The friction was calculated in the same way as for the wing and the tailplane, by treating the fin as a flat plate and taking account of the effect of sweep by the method of Ref.14.

(b) Wave drag

Estimates of wave drag were made by referring to standard charts or equations, all of which were derived from linearised theory.

The wave drag of the von-Karman ogive is, according to linear theory, independent of Mach number and is a very simple function of its slenderness ratio[15]. The wave drag of the afterbody was equated to that of the nose in accordance with Fraenkel's reversibility theorem[16]; the wave drag due to interference between the nose and the afterbody was estimated by using R.Ae.S. data sheet bodies S.02.03.10, which is based on an approximation in Ref.16.

Appendix 3

The wave drag of the fin and tailplane was estimated by using the charts in Ref.17. These relate to wings with double-wedge sections, and the values obtained from them were factored to account for the sections used on the models. The factor for the hexagonal section of the fin was obtained by comparing the calculated wave drag of such a section with that of a double-wedge, in two-dimensional flow. The factor for the round-nosed aerofoil section of the tailplane was obtained by comparing experimental measurements.

Though the wing wave drag was not expected to develop fully at the Mach numbers of the free-flight tests, some indication of its magnitude was needed. For this purpose the wave drag of an equivalent straight-tapered wing was found by the method used to find the wave drag of the tailplane. The work of Brebner and Lord[18] suggests that this estimate will not be unrealistic.

To obtain the estimated values of the zero-lift wave-drag factor K_o (Fig.14) the wave drag of each wing-body combination was calculated by means of linear theory, using the numerical method of Ref.15.

Printed in England for Her Majesty's Stationery Office by the Royal Aircraft Establishment, Farnborough. W.T.60 K.4.

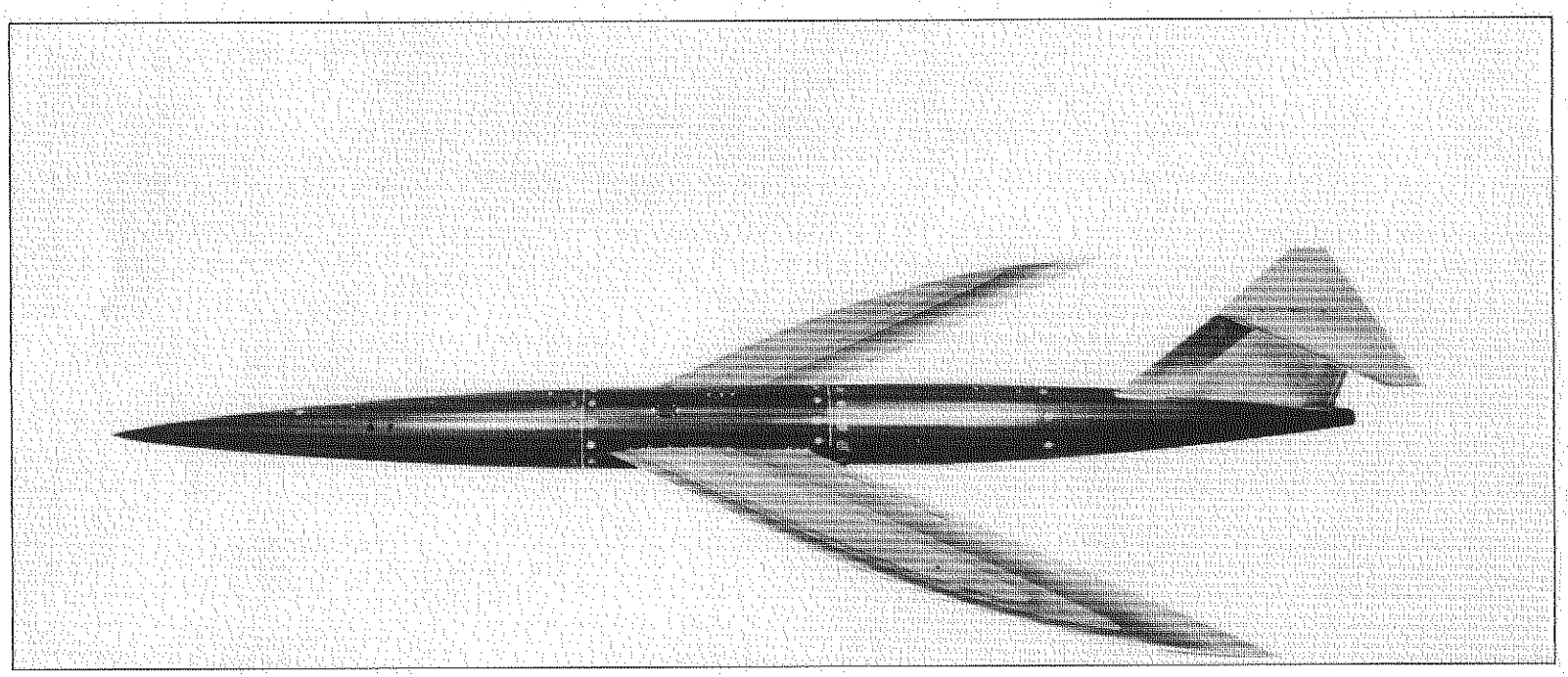

FIG.1. BASIC MODEL CONFIGURATION

WING SECTION RAE 101	(t/c = 0 06)
GROSS WING AREA	3 10 SQ FT
GROSS ASPECT RATIO	3 40
$\bar{\bar{c}}$ (GROSS WING)	0 985 FT

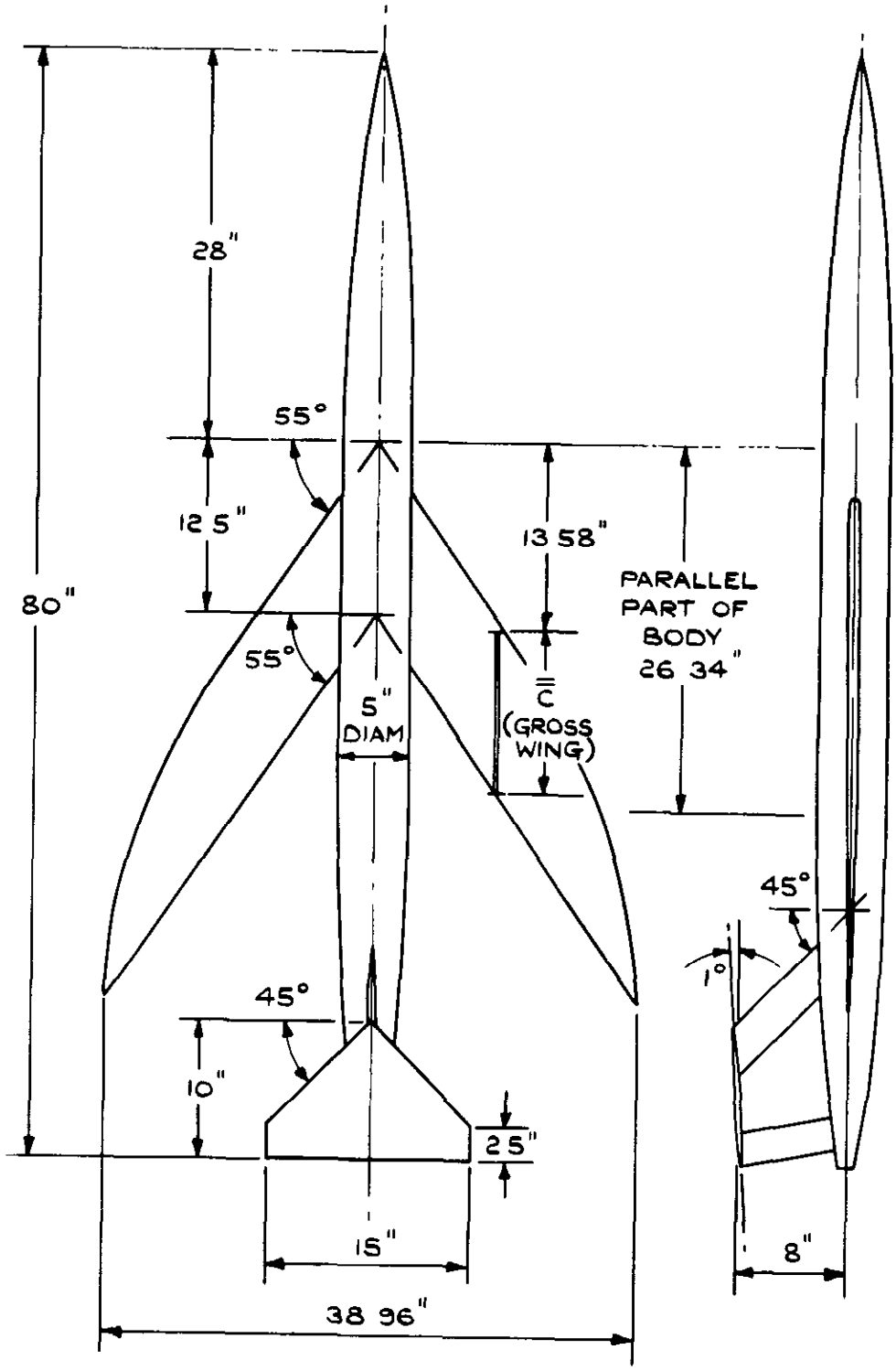

FIG 2. GENERAL ARRANGEMENT OF THE BASIC CONFIGURATION.
(CONFIGURATION No.1.)

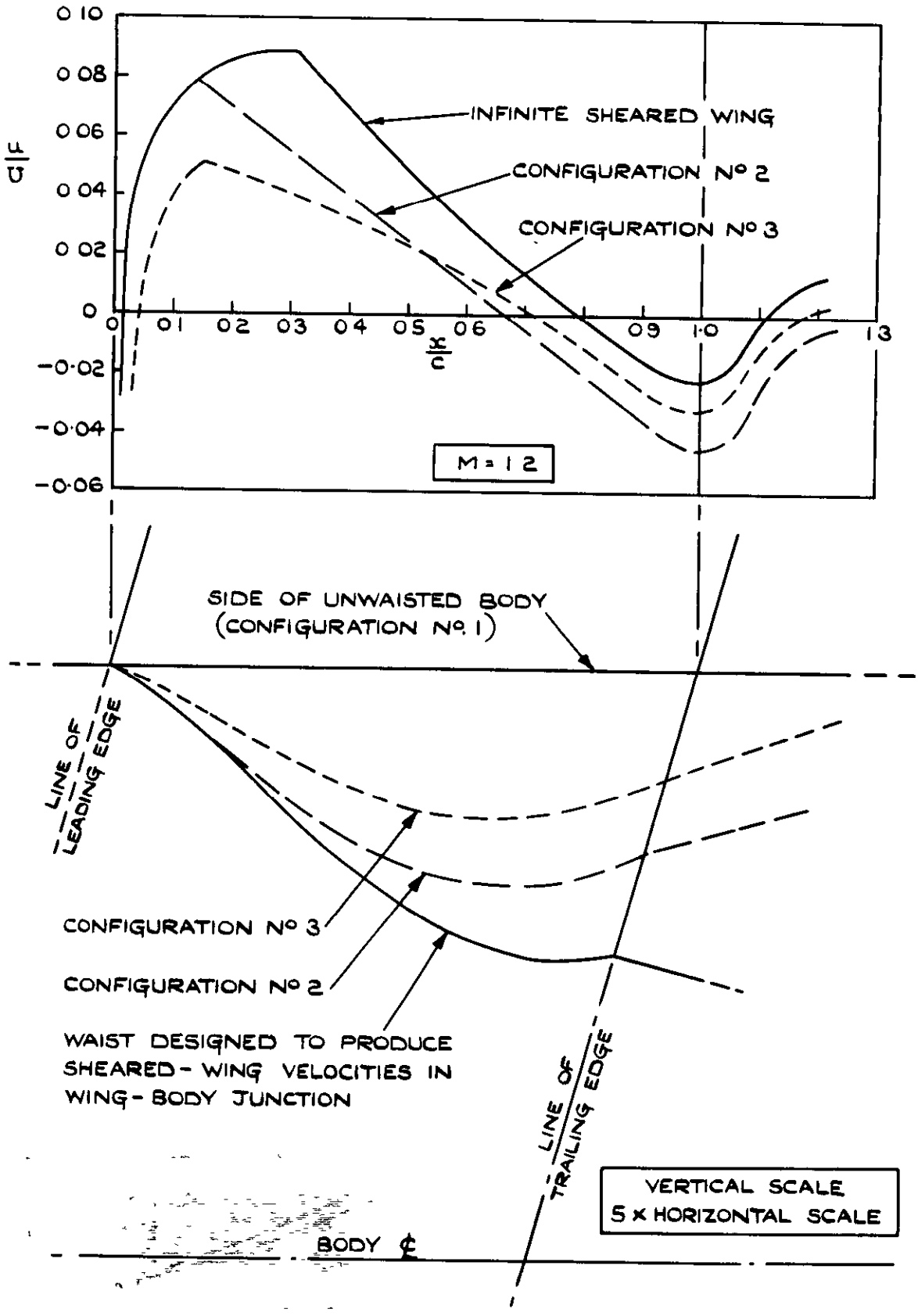

FIG. 3. PRESCRIBED JUNCTION VELOCITIES, AND BODY WAISTS DESIGNED TO PRODUCE THEM.

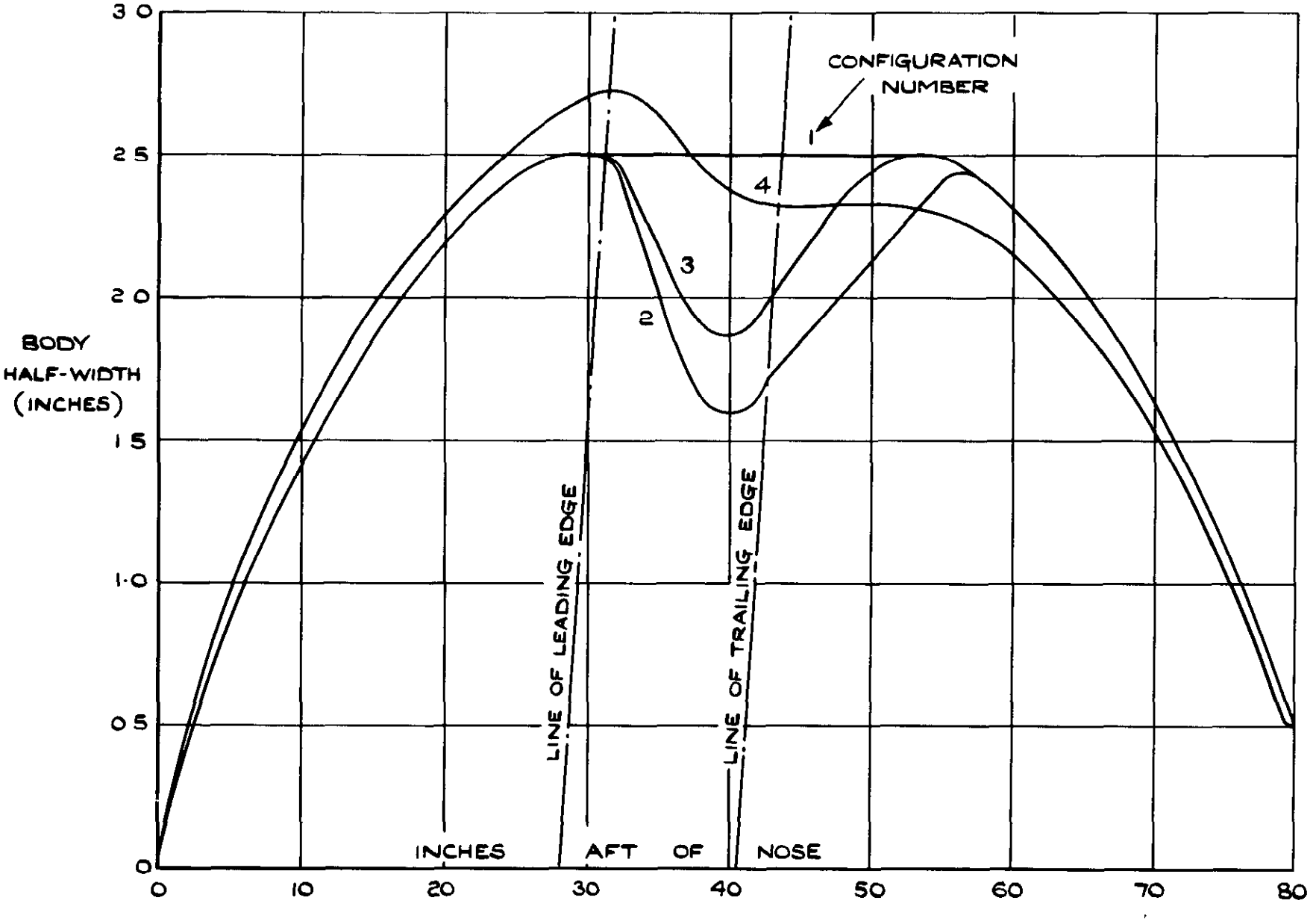

FIG. 4. COMPARISON OF BODY PLANFORMS.

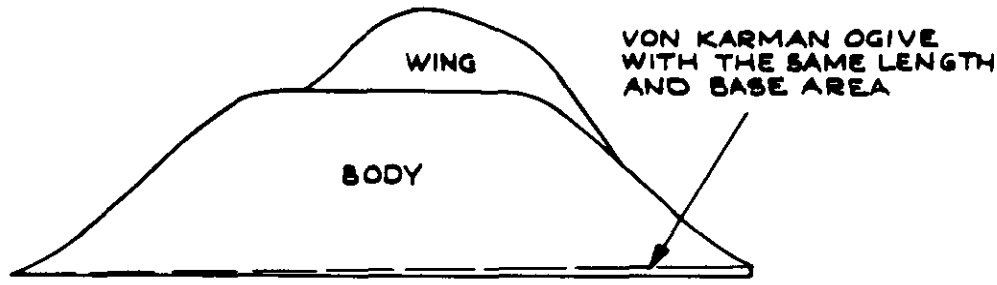

(a) THE BASIC, UNWAISTED WING - BODY COMBINATION.

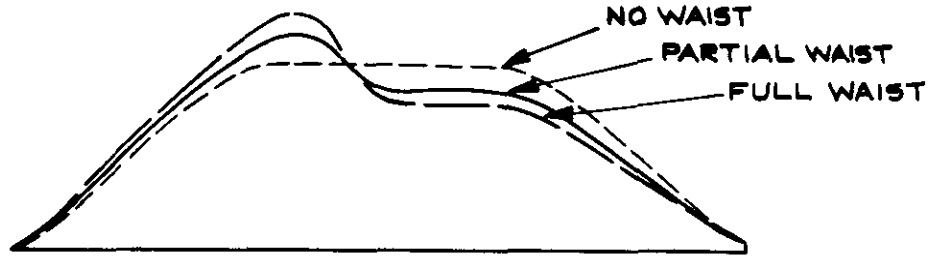

(b) DEVELOPMENT OF THE PARTIALLY - WAISTED BODY.

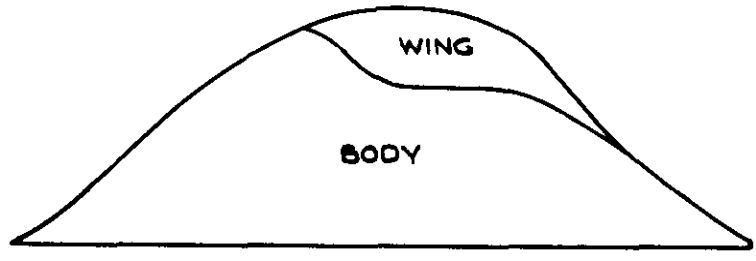

(c) CONFIGURATION No. 4

FIG. 5. NORMAL CROSS-SECTION AREA DISTRIBUTIONS SHOWING THE EVOLUTION OF CONFIGURATION Nº 4 (TAIL UNIT OMITTED)

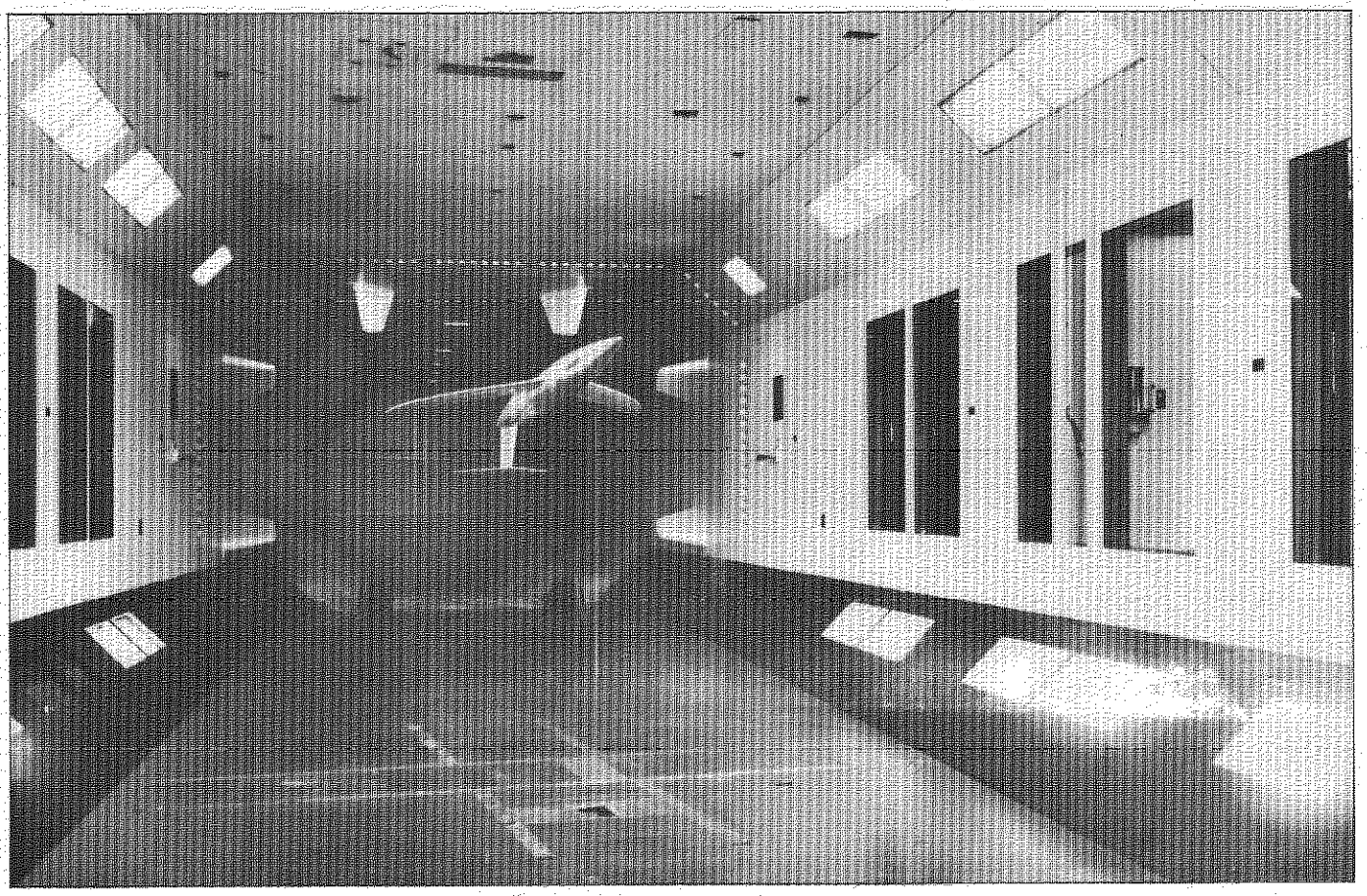

a. MODEL INSTALLED IN THE 13ft x 9ft WIND TUNNEL AT R.A.E. BEDFORD PRIOR TO FREE-FLIGHT TESTING

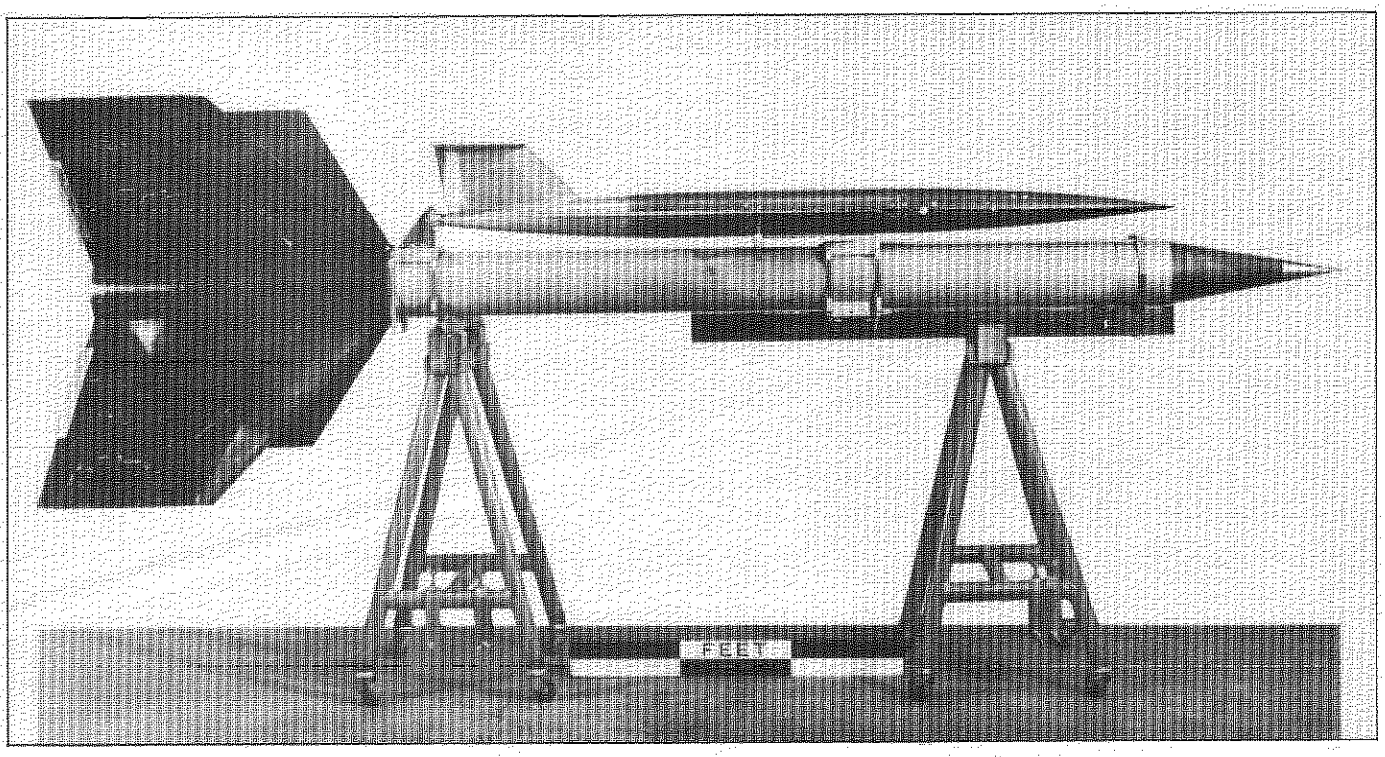

b. THE SAME MODEL WITH ROCKET MOTORS ATTACHED, READY FOR FREE-FLIGHT TESTING. PART OF THE BODY HAS BEEN ANODISED BLACK, TO FACILITATE VISUAL TRACKING

FIG.6a & b. ILLUSTRATING EXPERIMENTAL TECHNIQUES

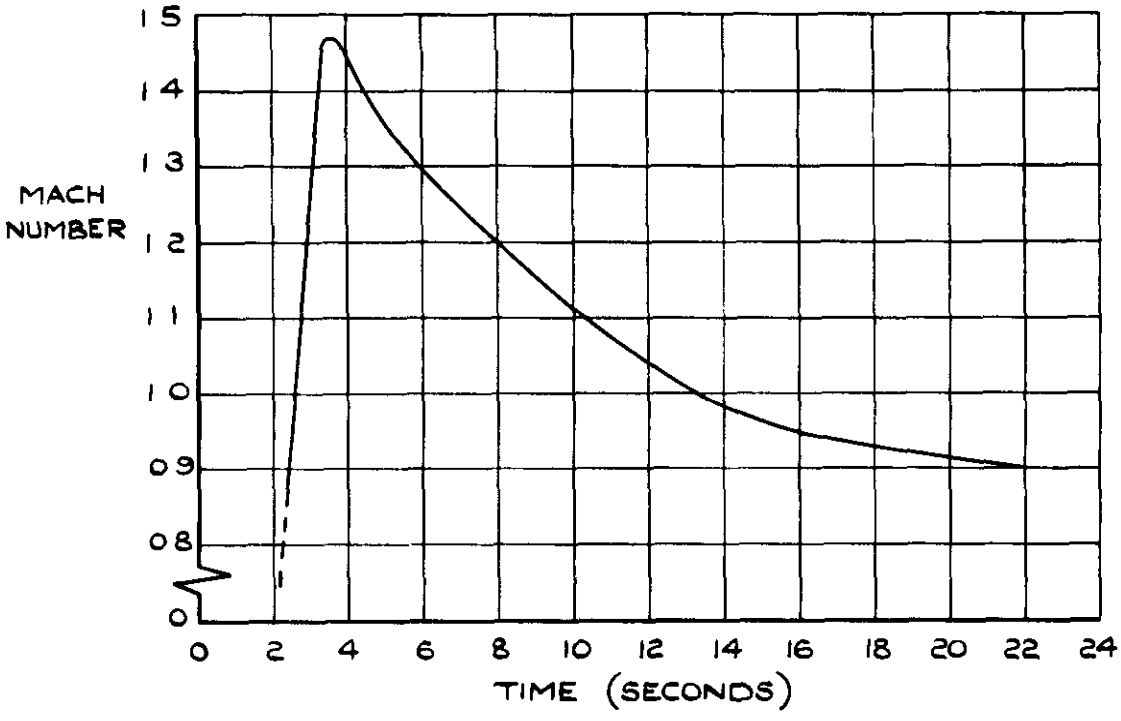

(a) TYPICAL VARIATION OF MACH NUMBER WITH TIME

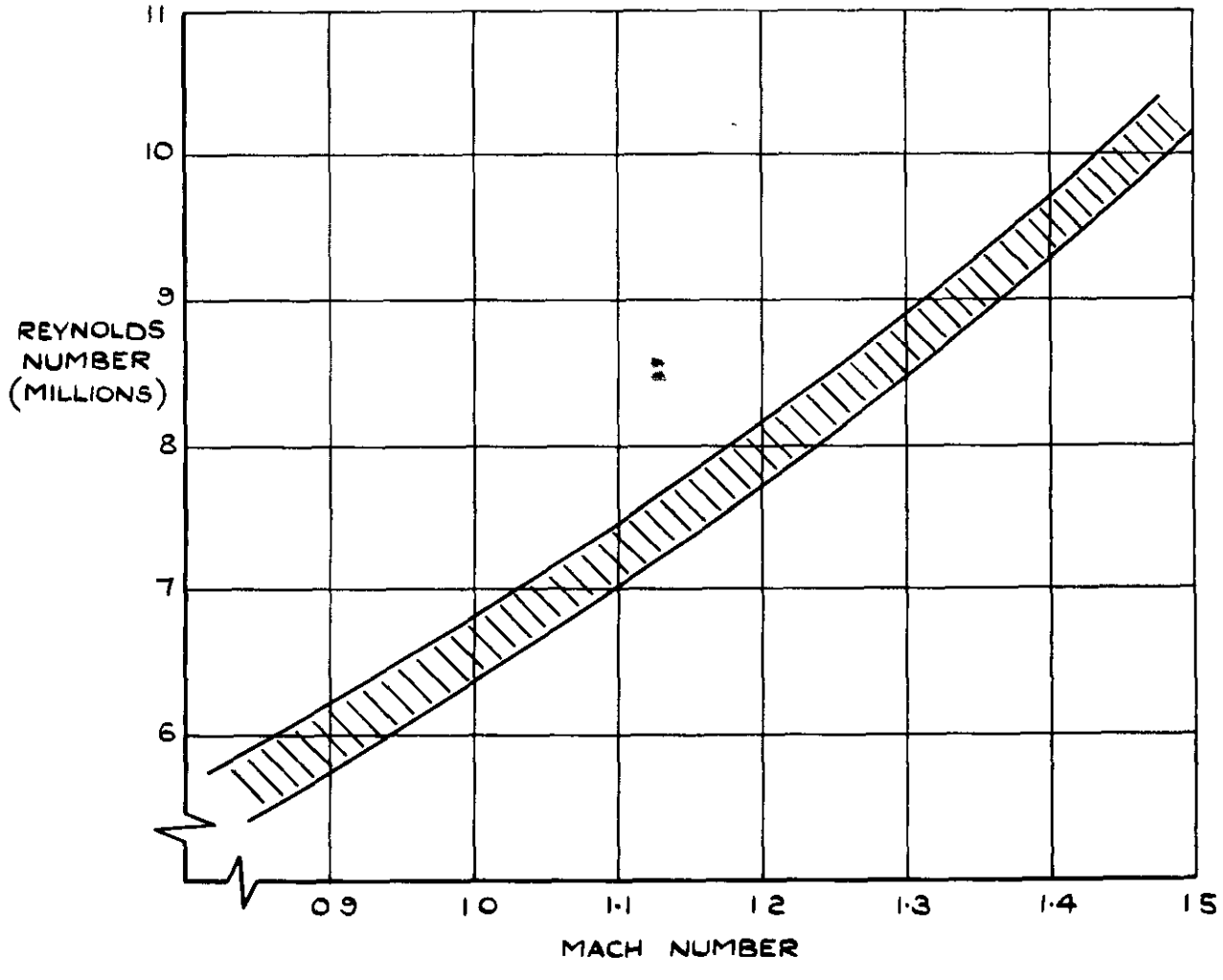

(b) VARIATION OF REYNOLDS NUMBER (BASED ON $\bar{c}$) WITH MACH NUMBER

FIG. 7. REYNOLDS NUMBERS AND MACH NUMBERS ACHIEVED IN FREE FLIGHT.

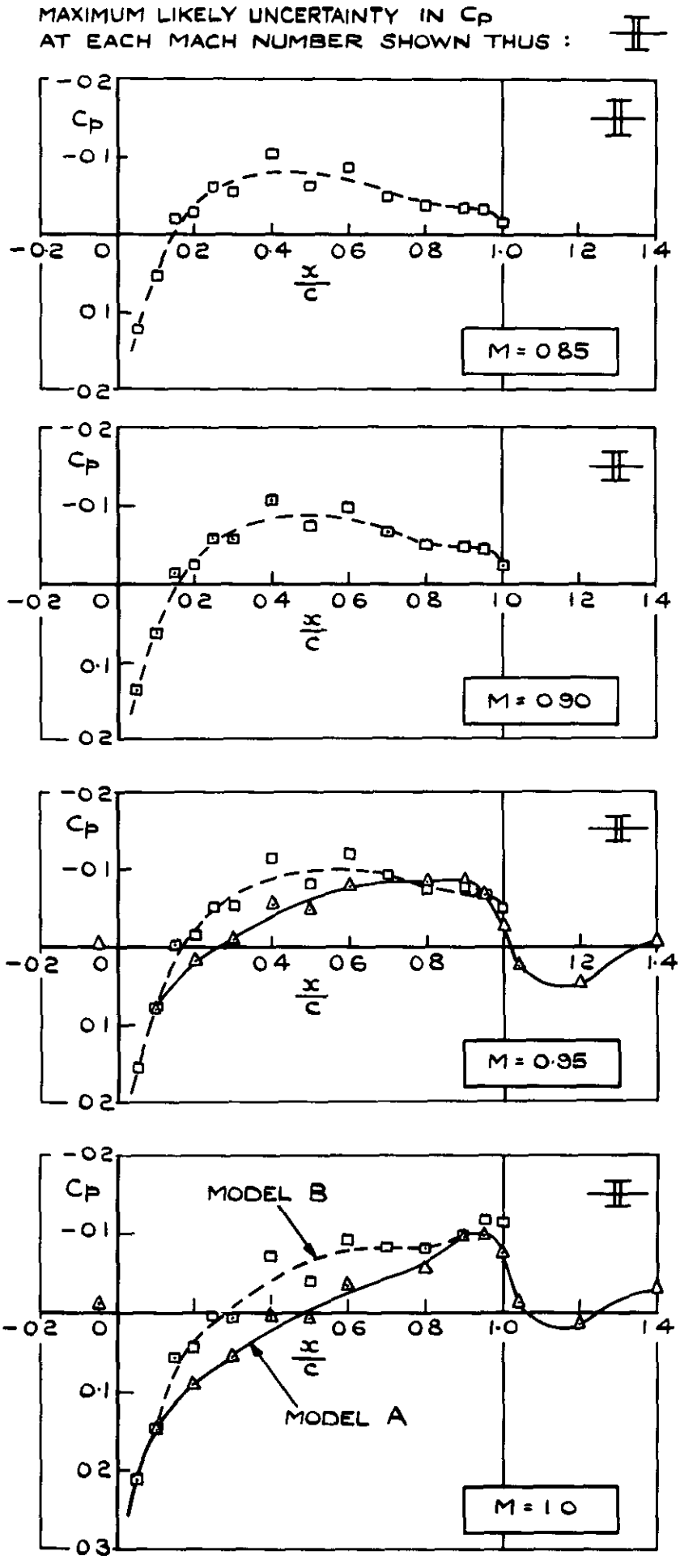

FIG. 8. PRESSURE DISTRIBUTION IN THE WING-BODY JUNCTION OF CONFIGURATION No. 1. (NO WAIST; 2 MODELS)

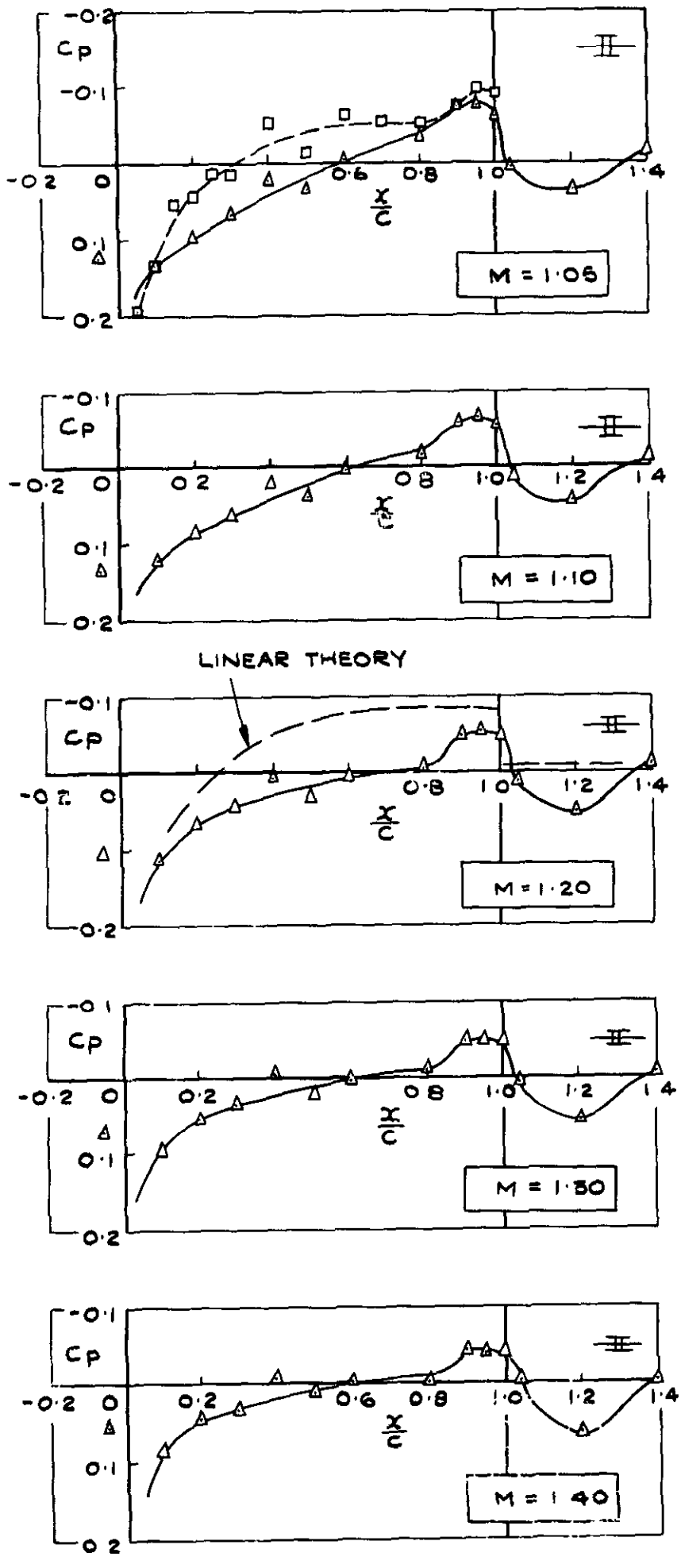
Cp
-0·2
-0·1
0·1
0·2
-0·2
0
0·6
0·8
1·0
1·4
x/c
M = 1·06
Cp
-0·1
0·1
0·2
-0·2
0
0·2
0·8
1·0
1·2
1·4
x/c
M = 1·10
LINEAR THEORY
Cp
-0·1
0·1
0·2
0·8
1·0
1·2
1·4
x/c
M = 1·20
Cp
-0·1
0·1
0·2
-0·2
0
0·2
0·8
1·0
1·2
1·4
x/c
M = 1·30
Cp
-0·1
0·1
0·2
-0·2
0
0·2
0·6
0·8
1·0
1·2
1·4
x/c
M = 1·40

FIG. 8. (CONCLD.)

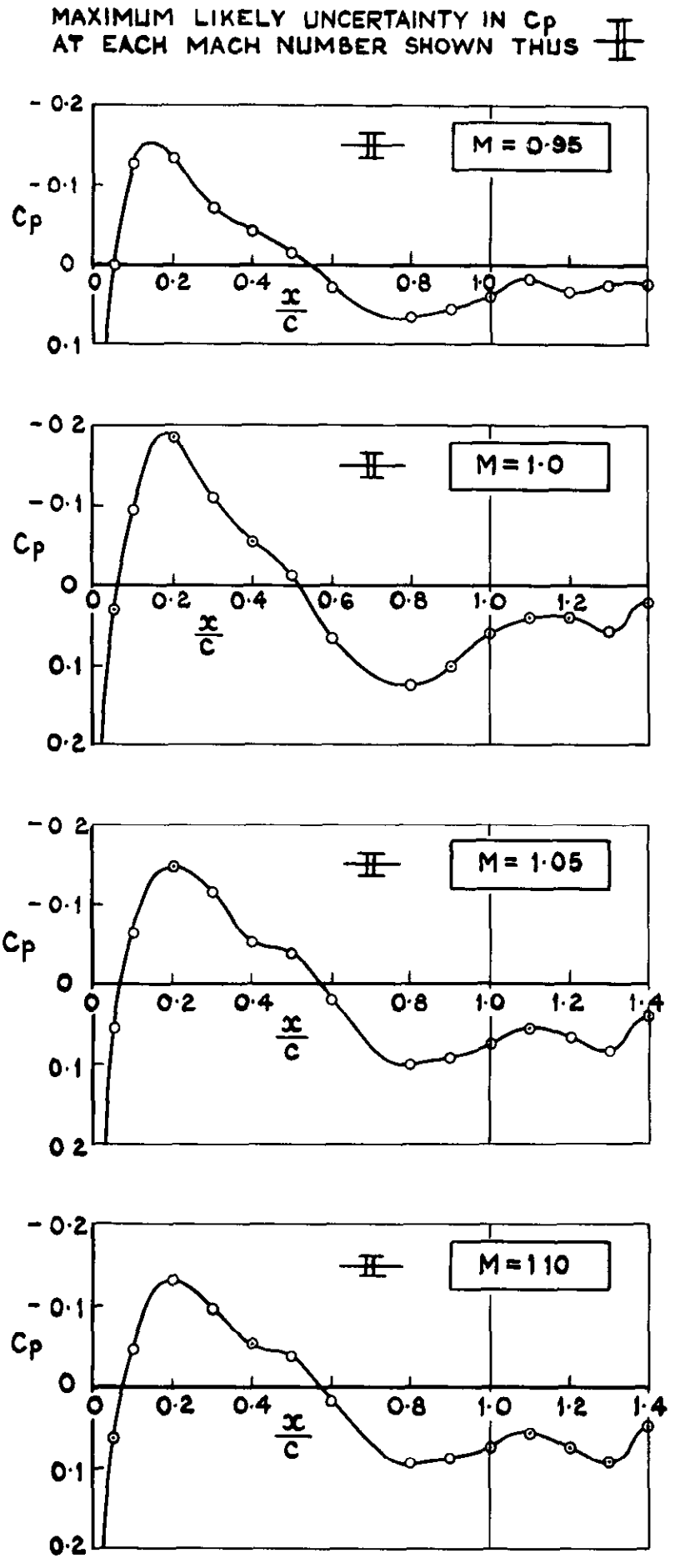

FIG. 9. PRESSURE DISTRIBUTION IN THE WING-BODY JUNCTION OF CONFIGURATION Nº. 2 (SEVERE WAIST)

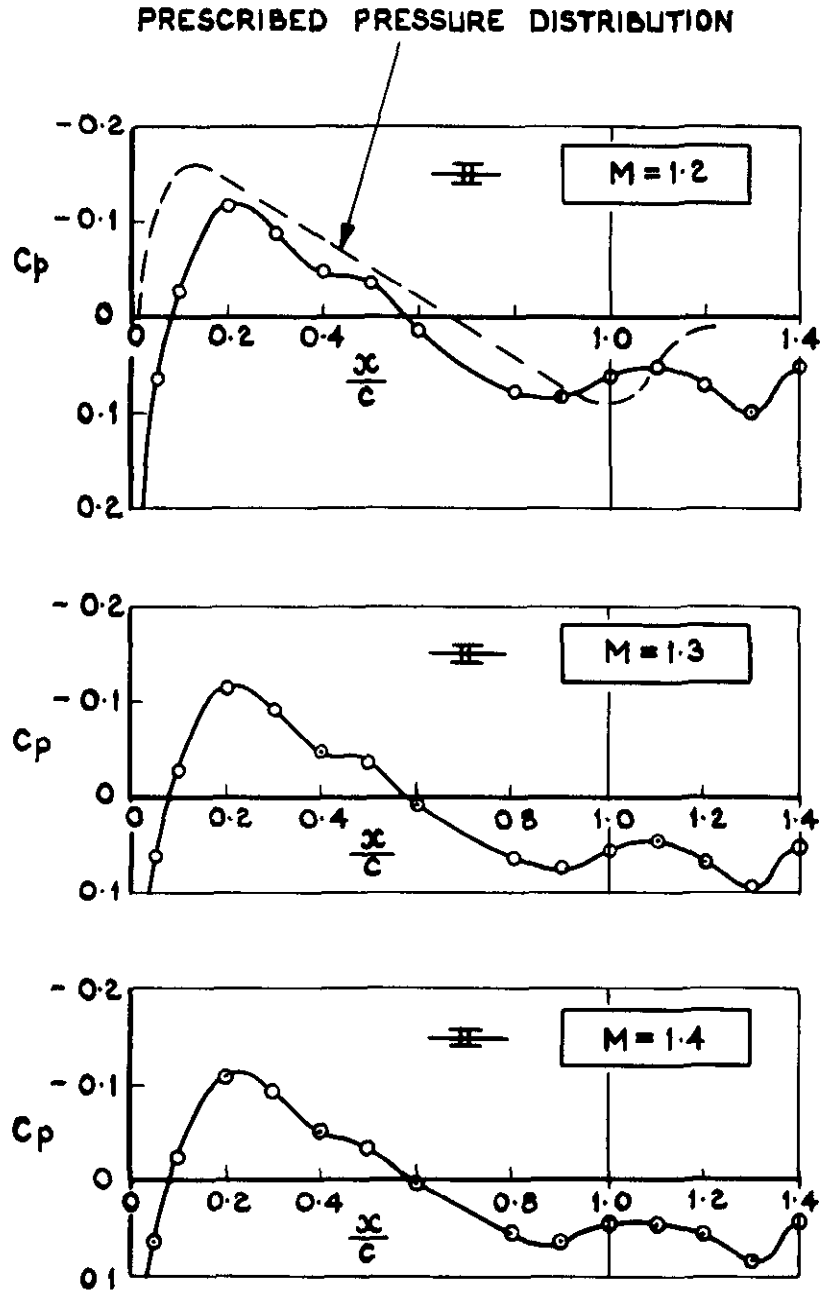
PRESCRIBED PRESSURE DISTRIBUTION
M = 1·2
M = 1·3
M = 1·4
Cp
x/c
-0·2
-0·1
0
0·1
0·2
0·4
0·8
1·0
1·2
1·4

FIG. 9. (CONCLD)

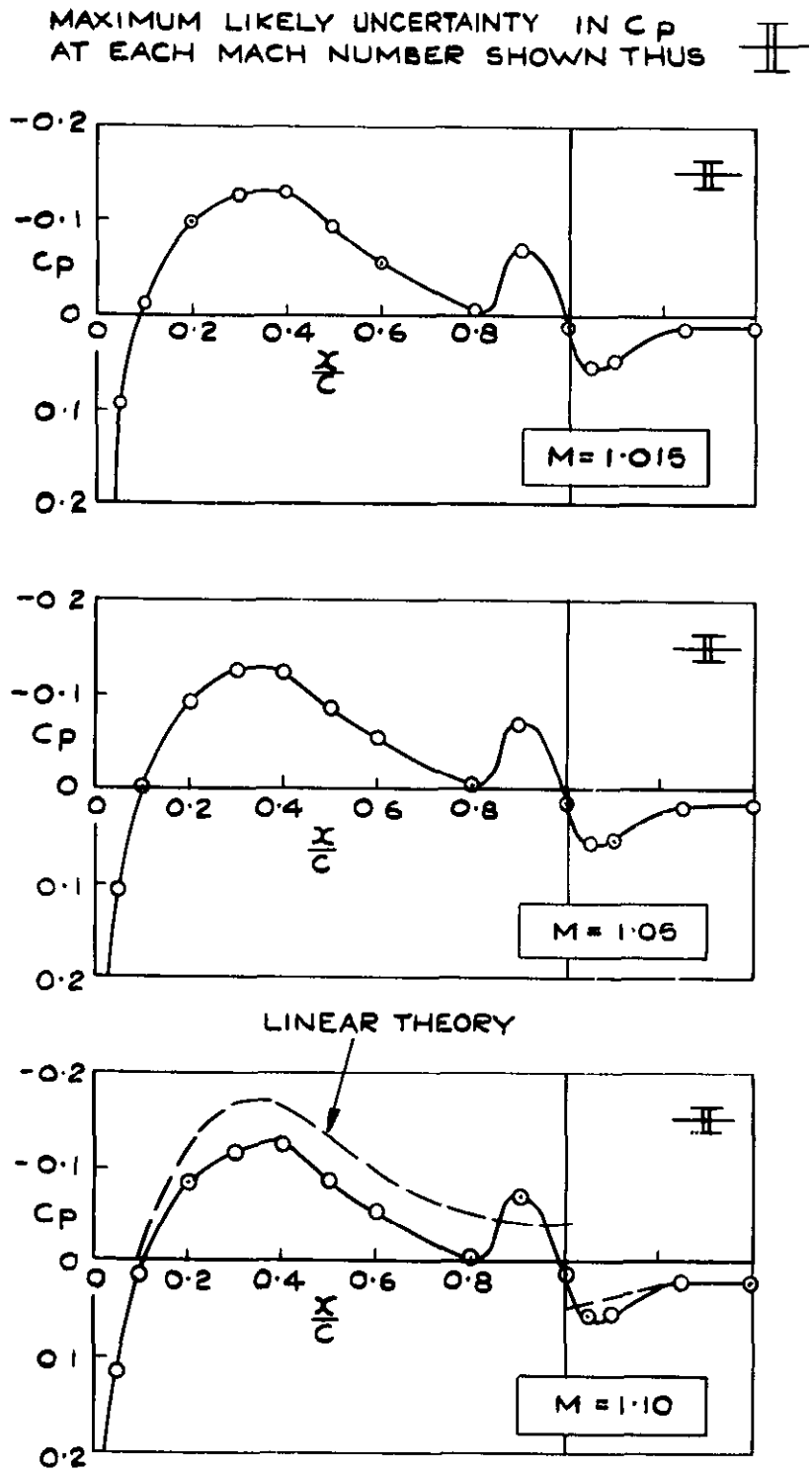

FIG. 10. PRESSURE DISTRIBUTION IN THE WING-BODY JUNCTION OF CONFIGURATION Nº 4 (AREA RULE)

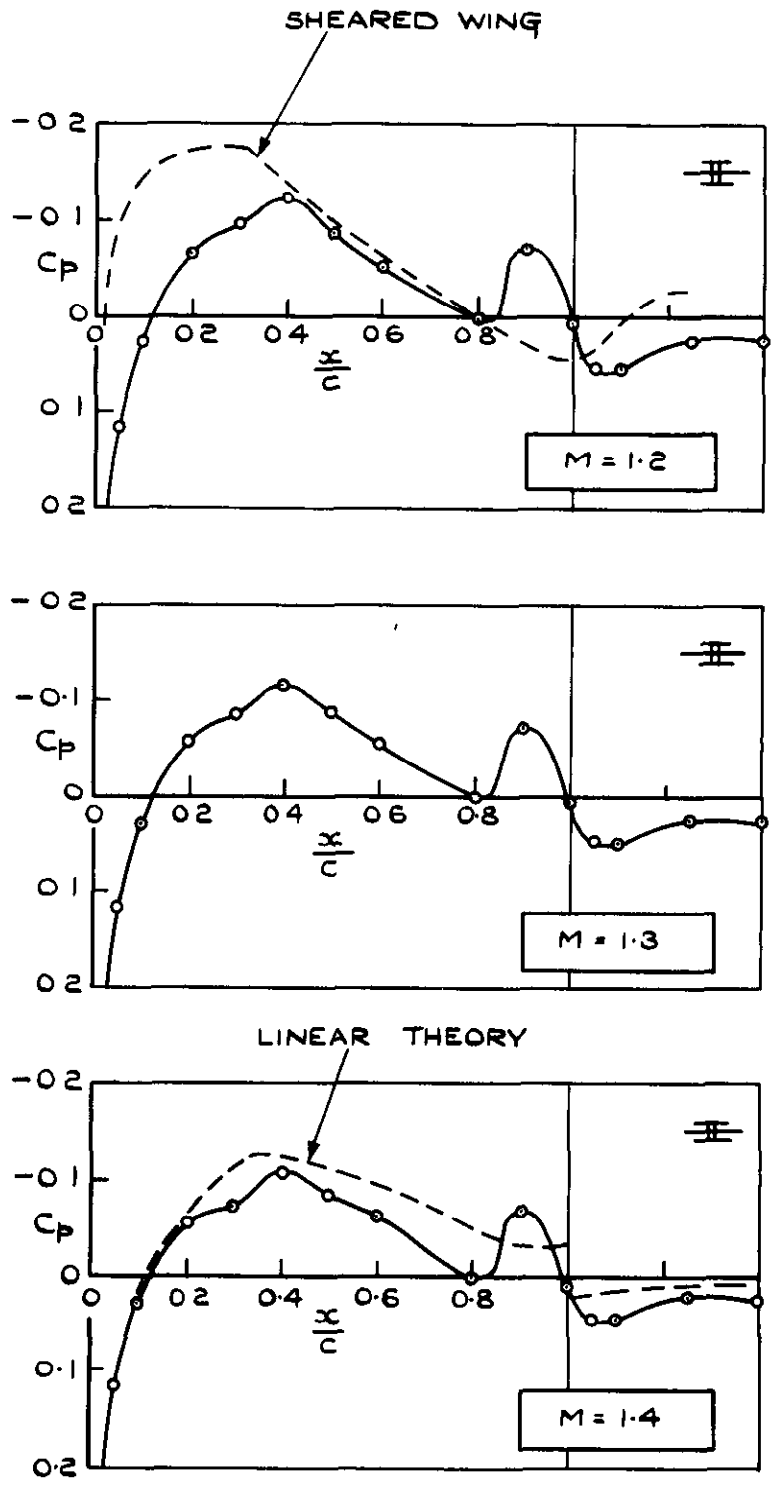

FIG. 10 (CONCLD)

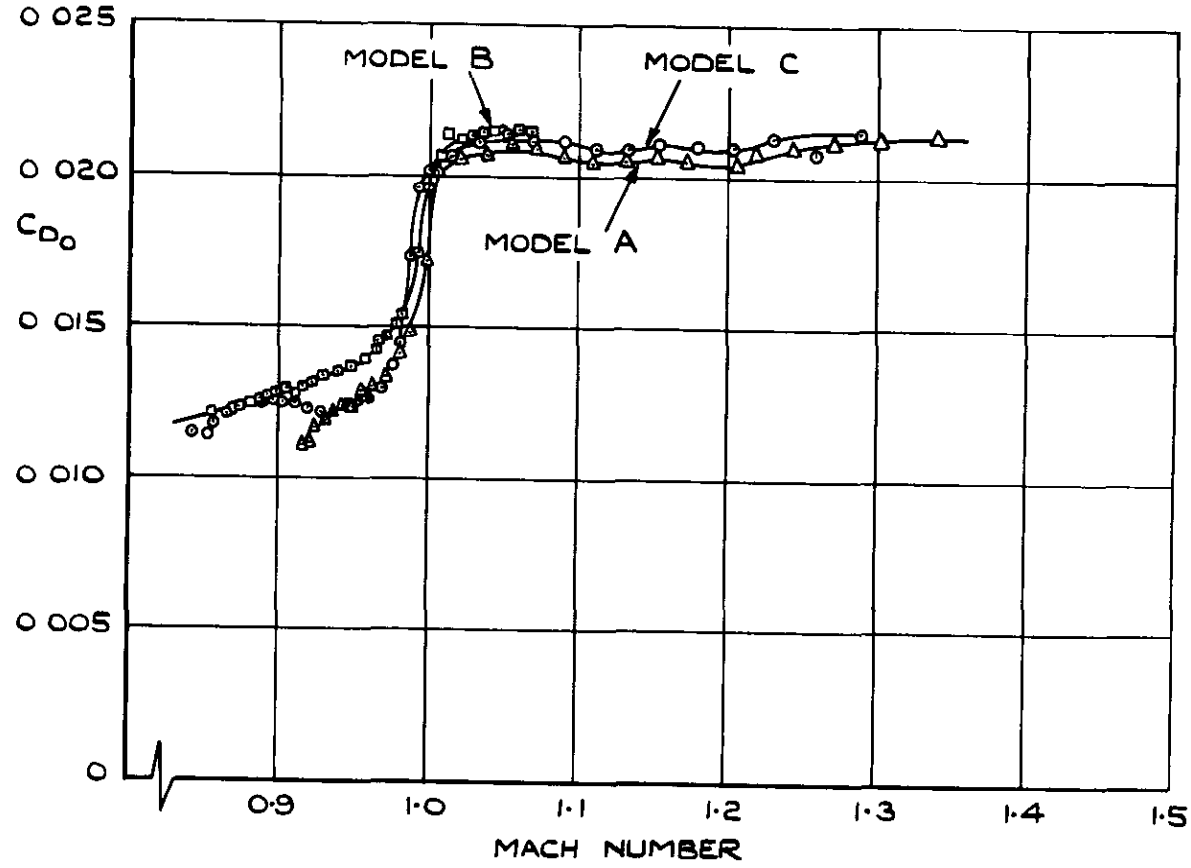

(a) CONFIGURATION No.1. (NO WAIST)

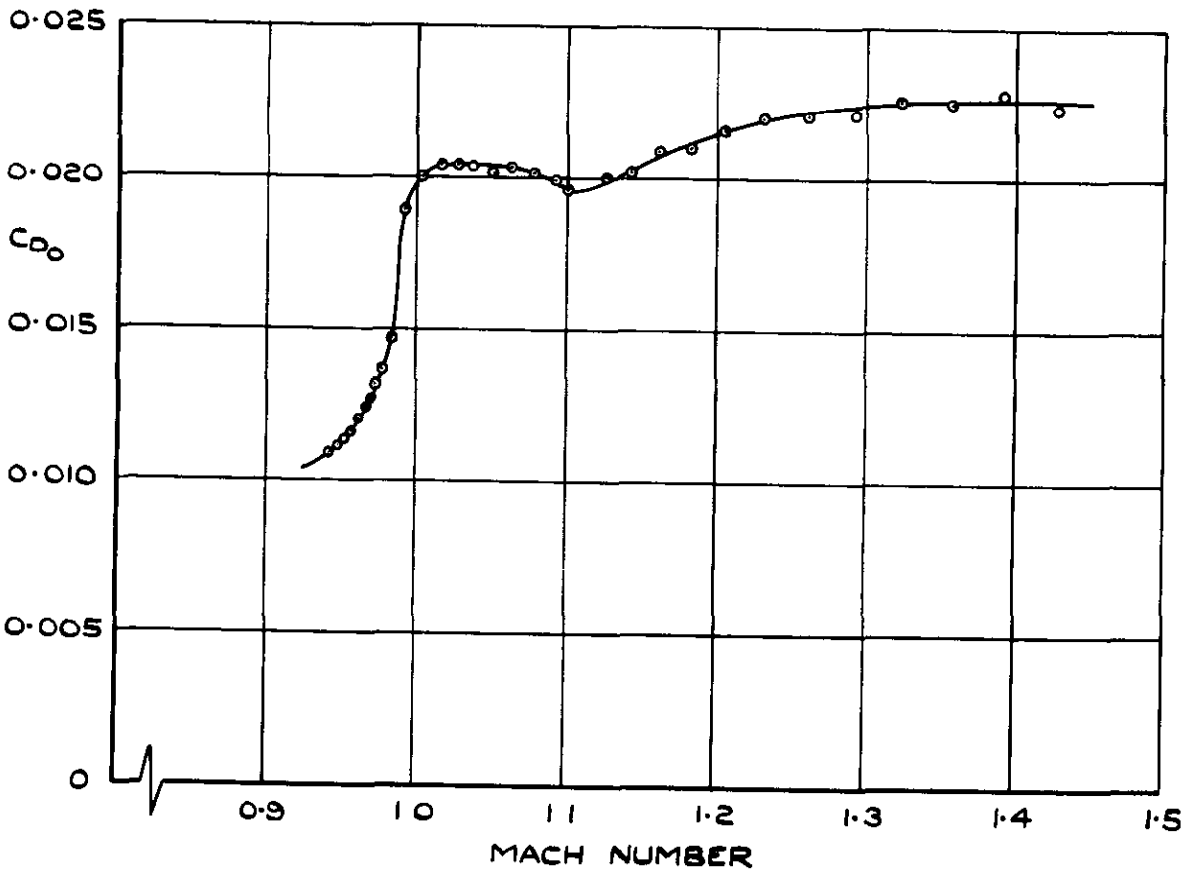

(b) CONFIGURATION No 2 (SEVERE WAIST)

FIG.11. MEASURED ZERO LIFT DRAG OF THE COMPLETE MODELS.

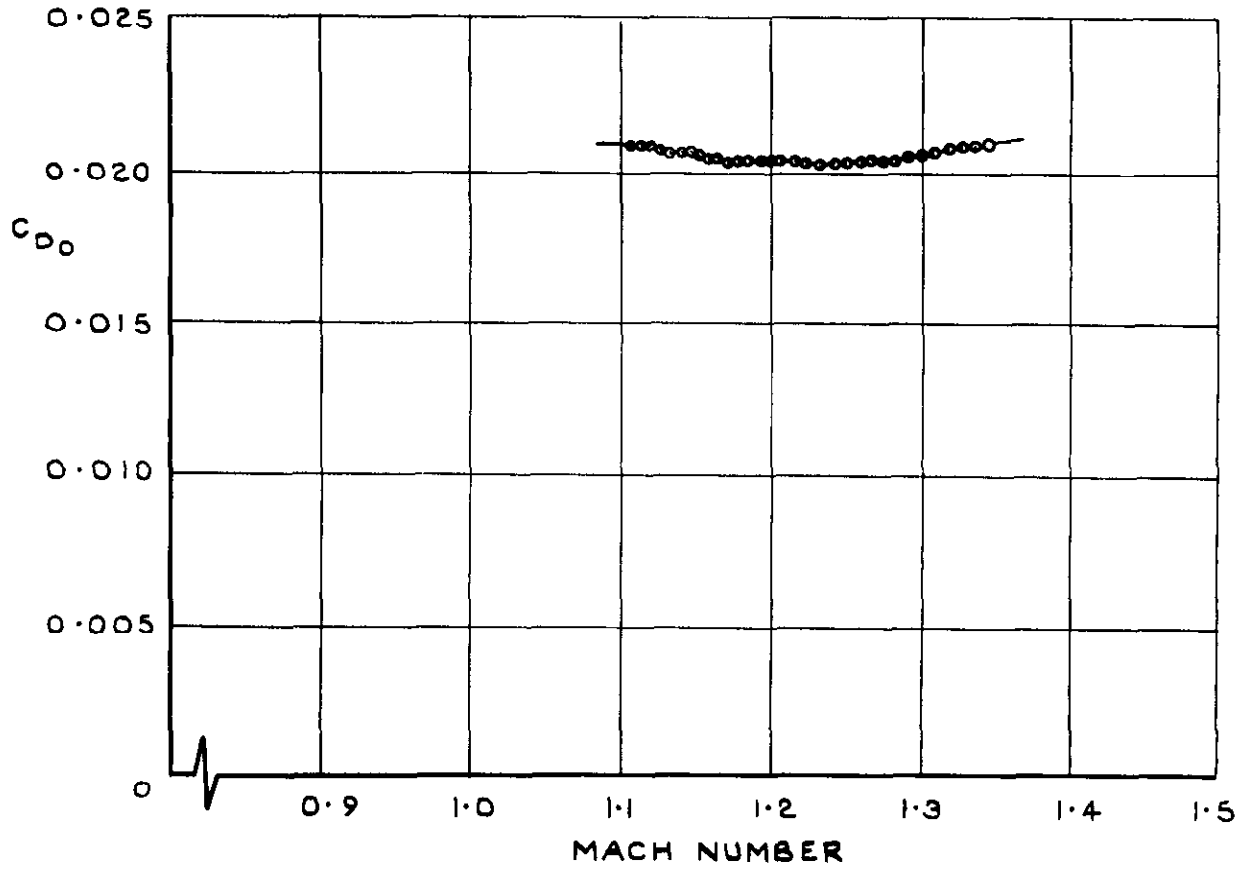

(c) CONFIGURATION No. 3. (MODERATE WAIST)

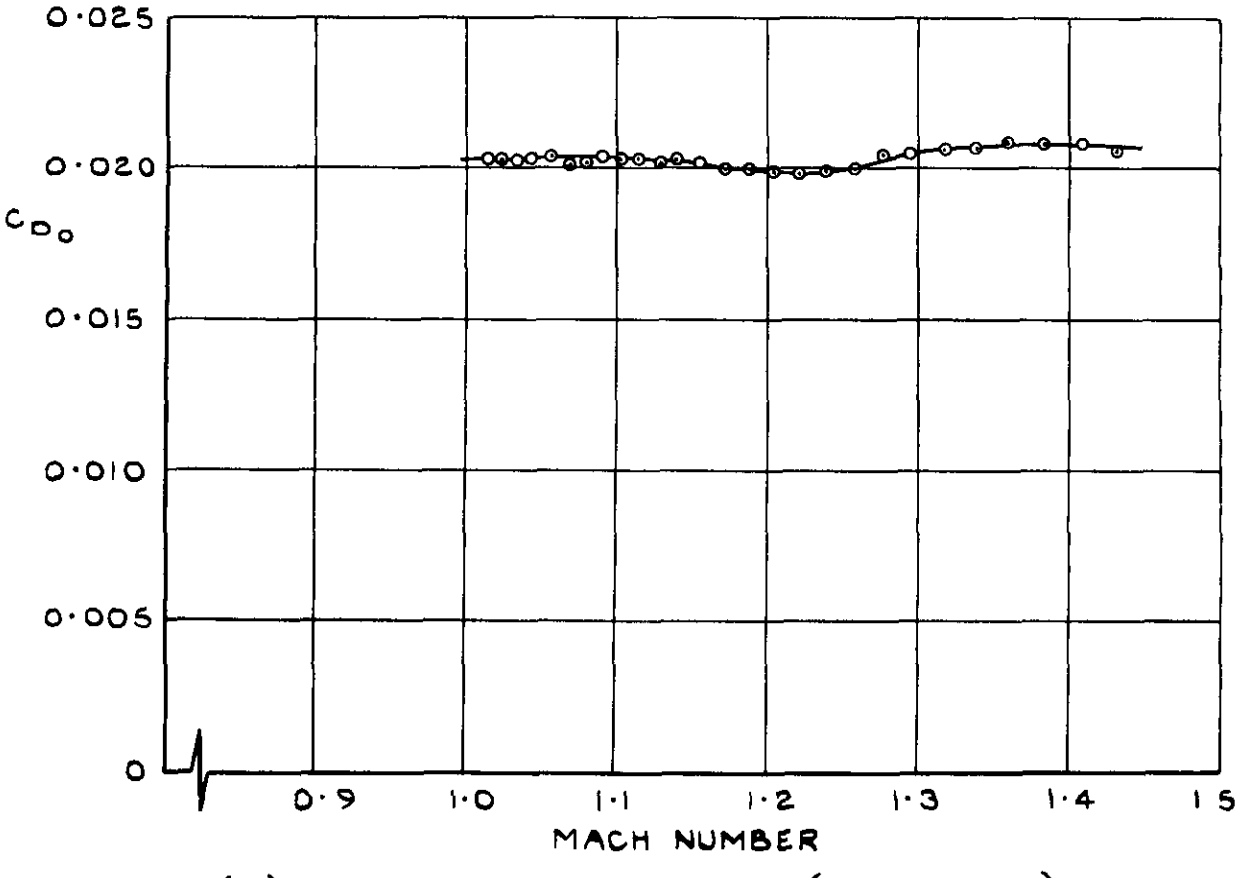

(d) CONFIGURATION No. 4 (AREA RULE)

FIG. 11. (CONCLD.)

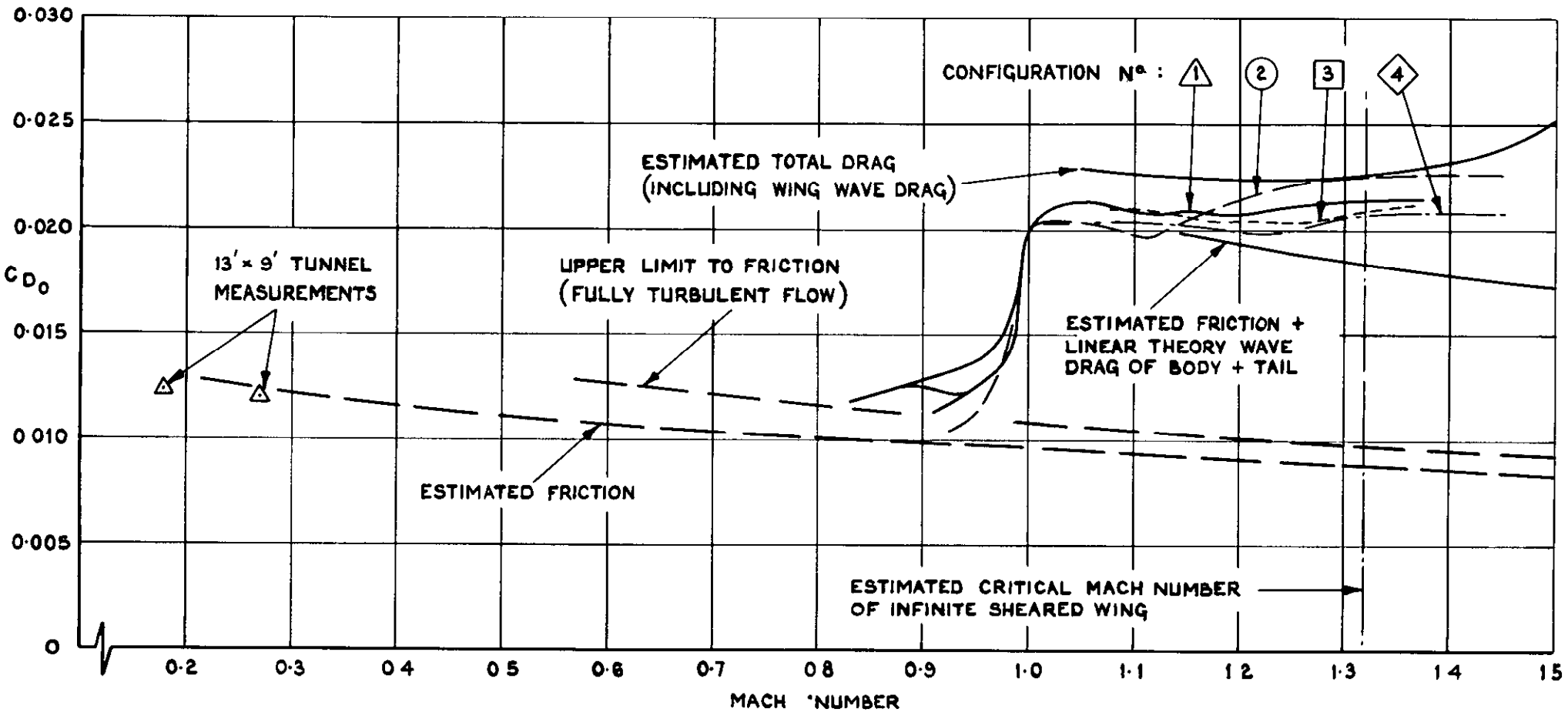

FIG.12. COMPARISON OF ZERO-LIFT DRAG MEASUREMENTS & ESTIMATES FOR THE COMPLETE MODELS.

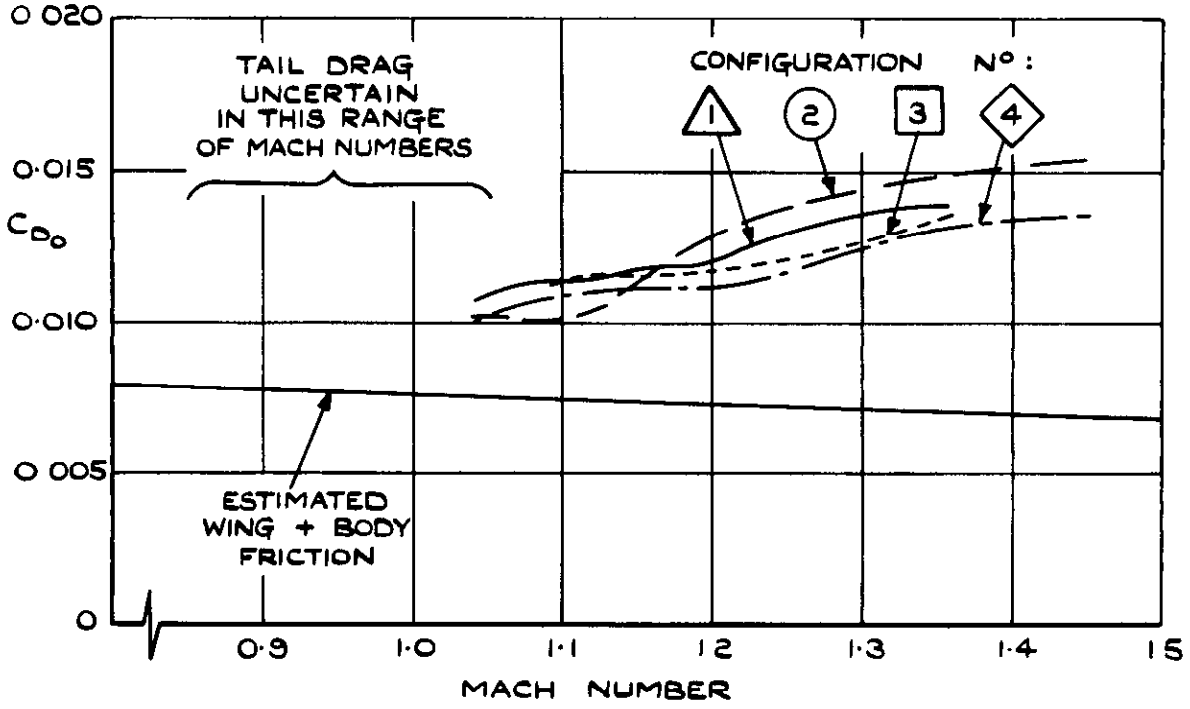

FIG.13. ZERO-LIFT DRAG OF THE WING-BODY COMBINATIONS.

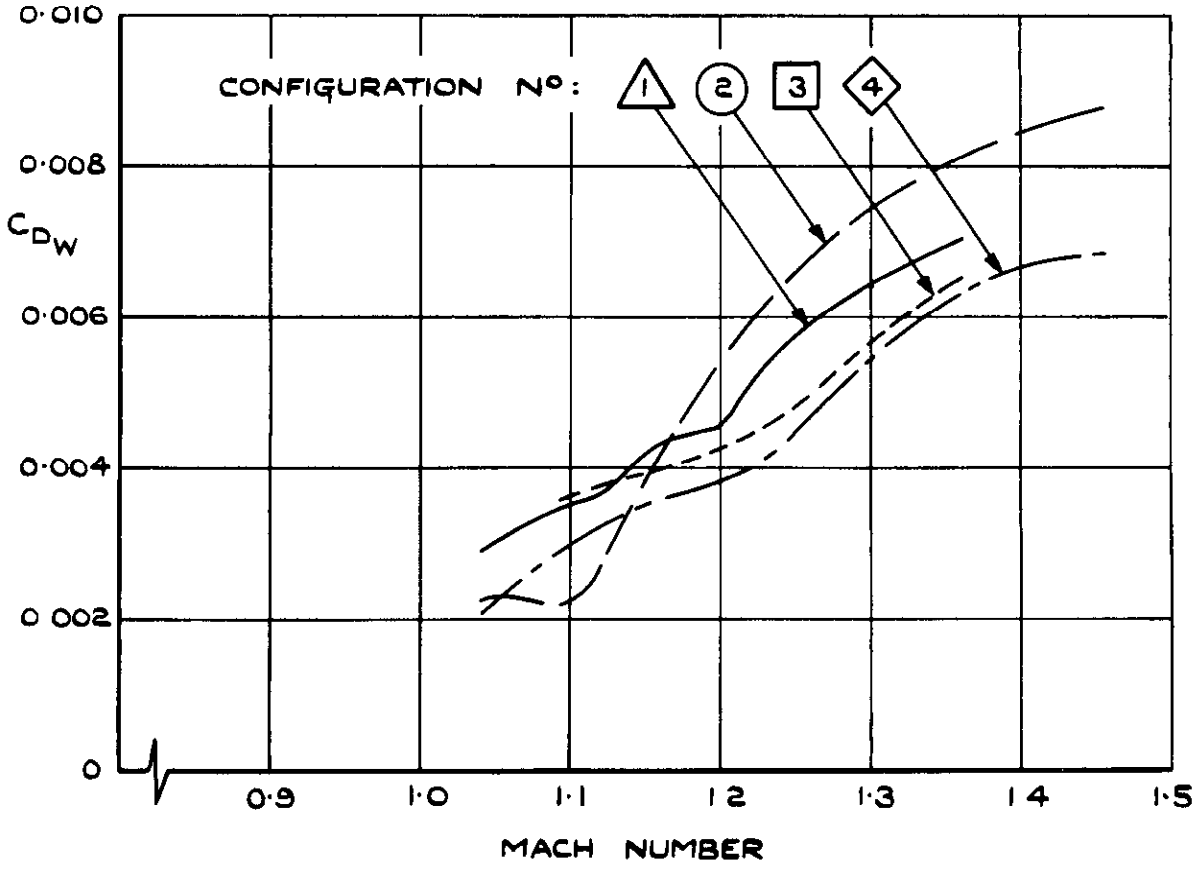

FIG.14. WAVE DRAG OF THE WING-BODY COMBINATIONS.

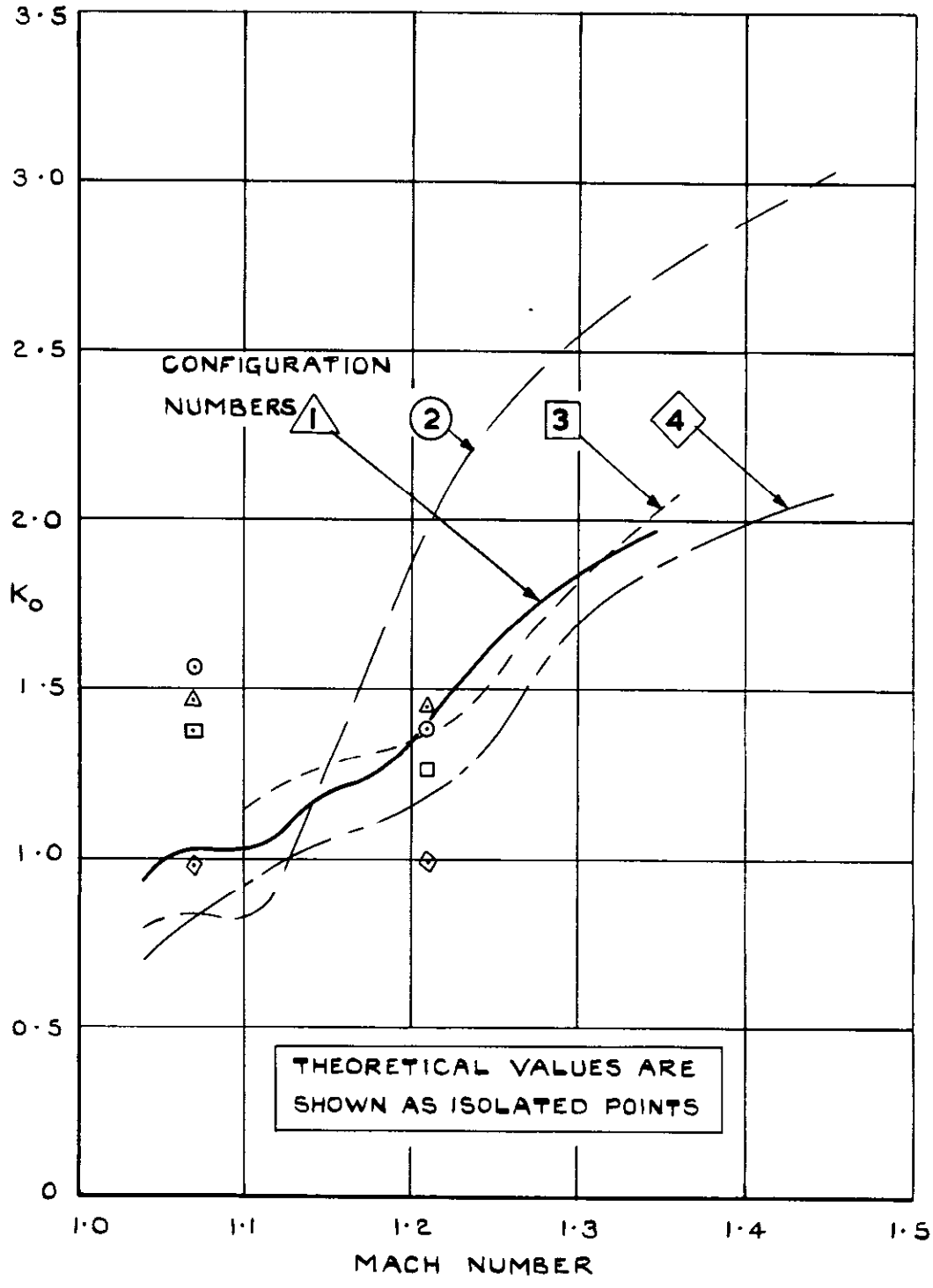

FIG. 15. ZERO - LIFT WAVE - DRAG FACTOR K_o FOR THE WING - BODY COMBINATIONS.

A.R.C. C.P. No.759

533.695.12:
533.6.013.122:
533.6.011.35

A FREE-FLIGHT INVESTIGATION OF WING-BODY JUNCTION DESIGN FOR A TRANSONIC SWEPT-WING AIRCRAFT. Hunt, G.K. August, 1963.

A method of designing the body of a swept wing-body combination, to obtain favourable wing-body interference at transonic speeds, has been investigated in free flight at zero lift. Models of four different bodies, in combination with identical wings swept back 55 degrees, were flown within the range of Mach numbers between 0.8 and 1.5 at Reynolds numbers, based on wing chord, up to 10 million. The general effectiveness of each body shape was determined by measuring the total drag of each model; the local effects of each design were determined by measuring the pressure distribution in the wing-body junction.

(Over)

A.R.C. C.P. No.759

533.695.12:
533.6.013.122:
533.6.011.35

A FREE-FLIGHT INVESTIGATION OF WING-BODY JUNCTION DESIGN FOR A TRANSONIC SWEPT-WING AIRCRAFT. Hunt, G.K. August, 1963.

A method of designing the body of a swept wing-body combination, to obtain favourable wing-body interference at transonic speeds, has been investigated in free flight at zero lift. Models of four different bodies, in combination with identical wings swept back 55 degrees, were flown within the range of Mach numbers between 0.8 and 1.5 at Reynolds numbers, based on wing chord, up to 10 million. The general effectiveness of each body shape was determined by measuring the total drag of each model; the local effects of each design were determined by measuring the pressure distribution in the wing-body junction.

(Over)

A.R.C. C.P. No.759

533.695.12:
533.6.013.122:
533.6.011.35

A FREE-FLIGHT INVESTIGATION OF WING-BODY JUNCTION DESIGN FOR A TRANSONIC SWEPT-WING AIRCRAFT. Hunt, G.K. August, 1963.

A method of designing the body of a swept wing-body combination, to obtain favourable wing-body interference at transonic speeds, has been investigated in free flight at zero lift. Models of four different bodies, in combination with identical wings swept back 55 degrees, were flown within the range of Mach numbers between 0.8 and 1.5 at Reynolds numbers, based on wing chord, up to 10 million. The general effectiveness of each body shape was determined by measuring the total drag of each model; the local effects of each design were designed by measuring the pressure distribution in the wing-body junction.

(Over)

The results show that it is possible to design a body which will produce a prescribed velocity distribution in the wing-body junction at a transonic design Mach number, but that it is necessary to control the velocity distribution elsewhere on the wing in order to ensure low drag. An adequate estimate of the overall wave drag is given by linear theory, provided that the Mach number is not too close to unity and the flow on the wing remains shock-free.

The results show that it is possible to design a body which will produce a prescribed velocity distribution in the wing-body junction at a transonic design Mach number, but that it is necessary to control the velocity distribution elsewhere on the wing in order to ensure low drag. An adequate estimate of the overall wave drag is given by linear theory, provided that the Mach number is not too close to unity and the flow on the wing remains shock-free.

The results show that it is possible to design a body which will produce a prescribed velocity distribution in the wing-body junction at a transonic design Mach number, but that it is necessary to control the velocity distribution elsewhere on the wing in order to ensure low drag. An adequate estimate of the overall wave drag is given by linear theory, provided that the Mach number is not too close to unity and the flow on the wing remains shock-free.

Published by
HER MAJESTY'S STATIONERY OFFICE

To be purchased from
York House, Kingsway, London w.c.2
423 Oxford Street, London w.1
13A Castle Street, Edinburgh 2
109 St Mary Street, Cardiff
39 King Street, Manchester 2
50 Fairfax Street, Bristol 1
35 Smallbrook, Ringway, Birmingham 5
80 Chichester Street, Belfast 1
or through any bookseller

S.O. CODE No 23-9015-59